Biomaterials Science

ROYAL SOCIETY OF CHEMISTRY

REVIEW

View Article Online
View Journal | View Issue

Cite this: *Biomater. Sci.*, 2025, **13**, 4639

Multifunctional bilayer dressings: a next generation biomaterial for enhanced wound healing

Dimpy Bhardwaj, Saurav Kumar and Garima Agrawal *

Wound healing poses a considerable challenge in the healthcare sector, especially for chronic and infected wounds, requiring advanced technological alternatives that surpass conventional dressings. Bilayer dressings, which combine hydrogels and electrospun nanofibers together, have recently emerged as a next generation biomaterial that mimics skin to enhance wound healing. Herein, we first describe skin physiology and various steps that are involved in the wound healing process. Based on this foundation, we further describe advancements made in individual hydrogel and electrospun nanofiber based single layer wound dressings and their *in vivo* implications. We discuss the shortcomings of these single layer dressings, and highlight the potential of bilayer dressings in overcoming these issues. Furthermore, we comprehensively elaborate the efforts made so far to develop bilayer dressings to advance skin wound care treatment. Finally, we discuss the challenges and opportunities existing in the area of bilayer dressings that should be addressed to achieve their clinical application in future.

Received 18th January 2025,
Accepted 9th July 2025

DOI: 10.1039/d5bm00095e

rsc.li/biomaterials-science

1. Introduction

Skin is the first defensive barrier which protects our body from invasion by foreign organisms and harmful substances. It has two primary layers: dermis and epidermis. Epidermis, ranging in thickness from 20 to 500 μm, is densely structured to protect against pathogens while maintaining breathability through numerous pores.[1] The dermis is primarily composed of fibroblasts and immune cells, which form a natural extracellular matrix (ECM) in combination with collagen and elastin.[2]

Small size skin wounds can heal by themselves by self-contraction; however, large size wounds caused by diseases or severe injuries require medical intervention to initiate the wound healing process.[3] Wounds are categorized as acute or

School of Chemical Sciences and Advanced Materials Research Centre, Indian Institute of Technology Mandi, Himachal Pradesh-175075, India. E-mail: garima@iitmandi.ac.in; Tel: +91-1905-267827

Dimpy Bhardwaj

Dimpy Bhardwaj is currently pursuing her Ph.D. at the School of Chemical Sciences at Indian Institute of Technology Mandi, India. She received her M.Sc. in Chemistry at Aligarh Muslim University, India in 2019 and completed her B.Sc. (Physics, Chemistry, and Mathematics) from Chaudhary Charan Singh University, India in 2017. She has qualified IIT JAM, CSIR NET-JRF, and GATE examinations. Her research focuses on the design and development of multifunctional polymeric biomaterials.

Saurav Kumar

Saurav Kumar completed his B. Sc. in Biotechnology from Patna Science College in 2021. He received his M.Sc. in Biotechnology at Rajiv Gandhi Centre for Biotechnology (RGCB), Thiruvananthapuram, India. Currently, he is pursuing his Ph.D. at IIT Mandi jointly under the supervision of Dr Garima Agrawal and Dr Yashveer Singh since 2024. His research focuses on designing polymers and peptide-based biomaterials for wound healing applications.

chronic based on the damage source and the duration of healing. Wounds caused by trauma or surgery are often acute wounds, while various infectious diseases, diabetes, or cancer lead to chronic wounds.[4] Chronic wounds are hard to heal over time. It has been estimated that almost 40 million people suffer from chronic wounds worldwide.[5] Furthermore, the annual expenditure for treating all kinds of skin wounds is estimated to be between $28 billion and $97 billion, leading to heavy financial burden on the healthcare sector globally.[6]

The biological process of wound healing involves repairing of damaged cells or tissues which takes place in four stages that occur in a coordinated manner for the development of a new ECM and the network of blood vessels for the healing of skin.[7,8] However, various factors such as the site of wound, malnutrition, lower immunity, age, stress, and comorbidities can further prolong the healing process.[9]

An ideal wound dressing should possess the following features: (a) biocompatibility, (b) protection from bacterial infection, (c) maintaining a moist environment, (d) required mechanical strength for having structural integrity, and (e) resemblance to skin physiology and ability to perform pro-healing biochemical actions (Fig. 1).[9] Gauzes and bandages are the most affordable traditional wound dressings. However, they are unable to protect the wound from getting infected by outside bacteria and maintaining the moist environment. Also, they cannot absorb the wound exudate and cause pain on removal as they stick to the wound site. Additionally, they might leave behind particles or fibers that trigger the immune system and cause formation of granulomas.[10] To address these issues, various interactive wound dressings (*e.g.*, transparent films, foams, hydrogels, and nanofibrous mats) have been reported so far.[5] In contrast to gauzes, interactive wound dressings exhibit dynamic interactions with the wound and help in promoting the healing. Such dressings are able to keep the wound moist, protect it from external bacterial invasion, and facilitate the formation of granulation tissue. However, these dressings are not adequate for infected chronic wounds.[11] To meet this challenge, bioactive dressings having inherent bioactive properties (*e.g.*, antibacterial and pro-angiogenic properties) have been explored.[12,13] Such dressings can deliver bioactive compounds and can substantially involve in the healing process for effective wound management.[4,5]

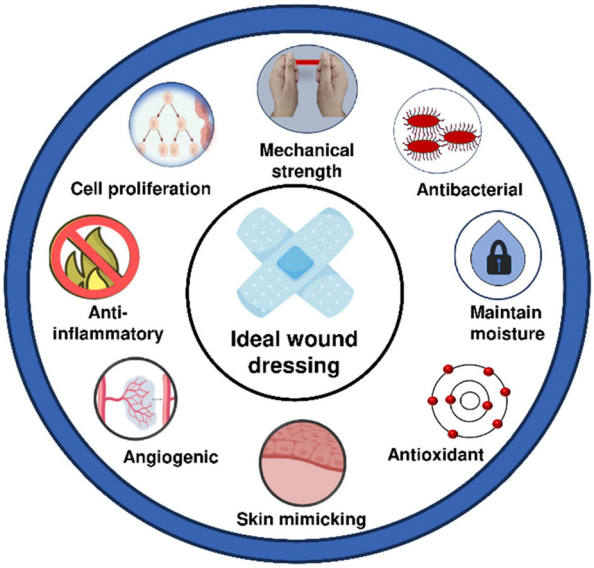

Fig. 1 Features required for an ideal wound dressing.

Taking a step further, in recent years, a considerable focus has been given to develop wound dressings that can mimic the skin. The concept of combining different biomaterials together to develop a bilayer matrix provides the opportunity to generate wound dressings that have structures similar to the epidermis and dermis.[7] Here, sponges and hydrogels can mimic dermal microstructures for supporting cell growth and to form the new ECM.[14] On the other hand, electrospun fiber mats can make a dense layer with small pores which is capable of protecting the wound from bacterial infection while maintaining the breathability.[14] However, this area of bilayer wound dressings is still in its infancy and requires significant attention to further improve the biochemical actions of these dressings.

This review presents an overview of bilayer dressings fabricated by combining hydrogels and electrospun nanofibers. Herein, we first discuss skin physiology, various stages of the wound healing process, and the limitations of conventional dressings, thus underscoring the necessity for further advancement. Next, we present recent developments in the case of both electrospun nanofibers and hydrogels along with their *in vivo* implications. Furthermore, we discuss the efforts made in the direction of developing bilayer dressings by integrating electrospun nanofibers and hydrogels together. We also focus on ECM-mimicking capabilities and active properties of bilayer dressings that promote wound healing. To conclude,

Garima Agrawal

Dr Garima Agrawal completed her M. Tech. in Polymer Science and Technology at the Indian Institute of Technology Delhi, India, and received her PhD at RWTH Aachen University, Germany, in 2015. She worked as a postdoctoral researcher at the University of Ghent, Belgium, and later as a DST Inspire faculty at IIT Roorkee. In 2019, she joined as an assistant professor at the School of Chemical Sciences, Indian Institute of Technology Mandi, India, where she is currently working as an associate professor. She is a recipient of NASI-Young Scientist Platinum Jubilee Award-2022, IIT Mandi Young Achiever's Award-2023, and DST Inspire Faculty Award-2016. Her research interests are in the fields of functional polymers, nanomaterials, and biomaterials.

we discuss the current shortcomings and potential future prospects for development in this area.

2. Skin physiology

Skin contributes to around 16% of body weight.[15] Its primary role is to protect the body from ultraviolet radiation, chemicals, and foreign bodies. It also helps to avoid depletion of essential body components like moisture and nutrients while simultaneously controlling blood pressure and detecting various stimuli.[15] It comprises three layers as discussed below.[16,17]

2.1. Epidermis

Epidermis, the first point of contact with the environment, is composed of keratin and epithelial cells arranged in tightly packed sheets. It is avascular and represents the thinnest layer of the skin. Various cells including keratinocytes, melanocytes, Langerhans cells, and Merkel cells build the epidermis, and help in protection and signal transduction. The epidermis is primarily made up of five distinct layers.[18,19] Stratum basale represents the innermost stratum of the epidermis. It is mainly made up of small round cells known as basal cells and melanocytes. Melanocytes produce melanin, which imparts a tan hue to our skin, which protects the deeper layers from the harmful effects of exposure to sun.[20] Stratum spinosum, the second layer, is built by 8–10 layers of keratinocytes. These cells are slightly flattened and closely connected by desmosomes. This connection enhances skin's strength and flexibility. Stratum granulosum, the third layer, consists of 3–5 layers of flattened keratinocytes. These keratinocytes undergo the process of apoptosis (*i.e.*, programmed cell death) as they move towards the surface of the skin. Stratum lucidum, the fourth layer, consists of 4–6 layers of flattened, transparent, and dead keratinocytes. Stratum corneum is the fifth and outermost layer consisting of 15 to 30 layers of cells. These layers are dry and dead, providing a mechanical barrier against microbe penetration and protecting the underlying tissues from dehydration. Periodically, cells move upward from the stratum granulosum to replace the shed cells in this layer.[21]

2.2. Dermis

Dermis, the second layer of skin, is responsible for providing the structure and flexibility to skin. It consists of two layers, namely the papillary layer and reticular layer. The papillary layer of the dermis establishes a connection between the dermis and epidermis through structures known as dermal papillae, which resemble finger-like projections. The papillary layer contains numerous small blood vessels, phagocytes, nerve fibres, arrector pili muscles and touch receptors (corpuscles). The reticular layer primarily consists of fibroblasts along with several glands and hair follicles. It imparts strength to the dermis along with ensuring its ability to stretch. The dermis has two primary functions: regulating temperature and transporting nutrient-rich blood to the epidermis.[22]

2.3. Hypodermis

The hypodermis or subcutaneous layer, the third layer of skin, is primarily found in areas where the body accumulates fat. It consists of adipose and fatty tissue. This layer is marked by the presence of significant blood arteries, nerves, and loose connective tissue. The adipose tissue of the hypodermis stores fat and keeps the body warm and comfortable. It serves as a protective layer against shock and trauma, conserves energy, and regulates the body's core internal temperature. Specialised connective tissue in the hypodermis links the dermis to muscles and bones within the body.[23]

3. Wound healing mechanism

Wound healing is a natural process that occurs in response to tissue damage resulting from injury, surgery, or disease.[24] The healing cascade consists of four steps which are described below.

3.1. Hemostasis

It helps in stopping the bleeding after vascular injury. It involves vasoconstriction and formation of platelet plugs which are followed by coagulation and reinforcement of the platelet plug.[25] Vasoconstriction *i.e.* constriction of blood vessel walls is the first response to a wound on skin, which stops the bleeding. Next, platelet aggregation and platelet plug formation take place, followed by the transformation of soluble fibrinogen into insoluble strands that generate fibrin mesh.[26] Thrombus, which is created by the combination of the fibrin mesh and the platelet plug, stops bleeding and releases growth factors while simultaneously acting as a temporary scaffold for the infiltration of cells required for wound healing.[27]

3.2. Inflammation

It is a complex biological process that attracts immune cells to the injury site to remove the debris and prevent infection. Injured or wounded cells emit molecules, which include chemokines, hydrogen peroxide (H_2O_2), damage-associated molecular patterns (DAMPs), and lipid mediators. These signals attract inflammatory cells, particularly polymorphonuclear leukocytes (PMNs). These inflammatory cells remove pathogens and cellular debris, and release inflammatory mediators such as TNF-α, IL-1, and IL-6.[28] These mediators activate the vascular endothelial growth factor (VEGF) and IL-8 for the healing process. Later, macrophages gradually replace PMNs and secrete cytokines that promote the recruitment of other leukocytes.[29] Once PMNs are eliminated, the macrophages undergo a phenotypic transition, transitioning from M1 macrophages to M2 macrophage. These M2 macrophages activate fibroblasts and keratinocytes, which eventually moves the process towards the proliferation phase.[30]

3.3. Proliferation

Here, the main aim is to fill the wound defect by neovascularisation, granulation tissue formation, and re-epithelialization.

Neovascularisation primarily occurs through angiogenesis and it is critical for nutrient transport, oxygen supply, and tissue regeneration.[31] Furthermore, granulation tissue, formed by activating fibroblast depositing collagen and ECM components, provides structural support for the healing process.[32] During the re-epithelialization process, peripheral cells proliferate and migrate, forming an epithelial layer that heals the wound.[33]

3.4. Remodeling

It is the final and most extended stage, lasting for months or even years. In this phase, several key processes contribute to complete tissue repair.[34] Collagen remodeling occurs as type III collagen is substituted by type I collagen, improving tensile strength and aligning fibers along tension lines to support the new tissue. The ECM undergoes continuous remodeling ensuring an equilibrium between degradation and synthesis. Furthermore, wound contraction, driven by myofibroblasts with contractile properties, occurs by pulling the edges together. As the tissue matures, collagen density and organization improve, thus increasing strength and elasticity. However, the repaired tissue remains less elastic and more prone to scarring than uninjured skin.[35]

4. Electrospun nanofibers

Electrospinning is a versatile technique for fabricating micro- and nanofibrous scaffolds from a variety of polymers by applying a high-voltage electric field to a viscoelastic polymer solution.[36] In the 16th century, Gilbert noted that when a solution was electrified, suspended droplets changed from a circular shape to a conical form due to an external electric field. This observation represented the initial conceptualization of what is currently referred to as electrospinning.[37] In 1915, Taylor further explored this phenomenon by formulating a mathematical model to illustrate the transition of a charged polymer solution from a circular configuration to a conical shape.[38] His research illustrated that the electric field applies a force on the charged droplet, elongating and distorting it. Upon attaining its critical tension, the droplet assumes a conical configuration and expels a linear jet from the apex of the cone. This unique conical formation is now designated as the "Taylor cone". The electrospinning process commences with the creation of a Taylor cone generating continuous fibers that accumulate as a fibrous mat on a grounded collector.[39] The resulting fiber morphology and mechanical behavior are influenced by various process parameters (such as the feed rate, applied voltage, and needle-to-collector distance), material properties (such as the molecular weight of the polymer, conductivity, and solution viscosity), and environmental factors.[40]

Some recent examples of electrospun nanofibers for wound healing, highlighting their characteristic features and *in vivo* implications, are summarized in Table 1. Various natural polymers such as gelatin (GL), collagen, chitosan, silk fibroin, dextran, hyaluronic acid, and alginate have been extensively explored for fabricating electrospun nanofibers owing to their inherent bioactivity, biocompatibility, and potential to promote tissue regeneration.[41–45] GL, which is derived from collagen, possesses excellent cell adhesion properties. This makes it a popular choice for creating wound dressings. GL nanofibers have been shown to absorb wound exudates efficiently while promoting macrophage activation, which is an essential process of wound healing.[46] In this direction, da Silva *et al.* reported the fabrication of aligned GL nanofibers crosslinked with glutaraldehyde.[41] These crosslinked GL nanofibers were coated with hyaluronic acid and utilized for the delivery of human corneal mesenchymal stem cells. *In vitro* experiments exhibited the ability of the system to support cell proliferation and migration. *Ex vivo* experiments performed using a rabbit model displayed reduced expression of α-smooth muscle actin (α-SMA) and enhanced regeneration of transparent stroma supporting corneal wound healing.

Similarly, chitosan, a naturally occurring polysaccharide, is widely recognized for its antibacterial properties and hemostatic potential.[47] Electrospinning of chitosan can be challenging due to its polyelectrolyte nature and poor solubility in water.[48] Researchers have addressed these issues by mixing chitosan with other polymers, which also enhanced the mechanical properties of the resulting nanofibers.[49] For example, Lungu *et al.* reported dual functionalized chitosan nanofibers loaded with 2 formylphenylboronic acid (2FPBA) and citral by employing a double imination mechanism.[50] Both the active compounds could be released by the degradation of imine bonds. Furthermore, it was observed that the release of 2FPBA was faster as compared to that of citral due to the hydrophilic nature of 2FPBA. Additionally, the antibacterial activity of 2FPBA was improved by the presence of citral, which enhances cell permeability and ROS production. This system demonstrated excellent antibacterial and antifungal effects for supporting wound healing.

Silk fibroin has been employed to create nanofibrous scaffolds with remarkable mechanical strength and biodegradability.[51] In this regard, Yang *et al.* reported silk fibroin/fibrin based electrospun nanofibers which showed excellent blood compatibility and appropriate biodegradation rates.[51] The fabricated nanofibers displayed balanced and controllable biomechanical properties, degradability, and good cell compatibility. Furthermore, electrospun silk fibroin nanofibers have been loaded with various therapeutic agents such as growth factors, demonstrating their potential to accelerate tissue regeneration and promote angiogenesis in chronic wound models.[52] Hyaluronic acid, a critical component of the ECM, is known for its role in moisture retention and facilitation of cell migration.[53] However, its high viscosity often complicates electrospinning. Blending hyaluronic acid with other natural polymers has also been explored to improve electrospinnability and cellular attachment, thus ultimately expediting wound healing.[54] It is to be noted that although natural polymers offer bioactive features to the electrospun nanofibers, their batch to batch variations caused by different sources (*e.g.*

Table 1 Recent advances in electrospun nanofibers for enhanced wound healing and their *in vivo* implications

S. no.	Nanofiber material	Active component	Remarks	Ref.
1	Chitosan/pectin/PVA	HDIC	HDIC incorporated nanofibrous membranes are biocompatible and antibacterial. Their anti-inflammatory properties regulate the wound environment polarising M2 macrophages. A sustained release of dihydromyricetin ensures long-term medicinal efficacy. HDIC release profile exhibits a distinct two-stage pattern involving initial burst release within the first 30 min, followed by a steady release (≈100%) over 120 min. Moreover, *in vivo* wound healing experiments demonstrate the nanofiber membrane's ability to speed up wound closure in the rat model.	Guo *et al.*[88]
2	Silk protein/PCL	PHL@CD	The incorporation of a PHL@CD complex into the wound dressing significantly improves its antibacterial and antioxidant characteristics. It helps in targeting two essential aspects of diabetic wound management: infection prevention and inflammation reduction. Moreover, fabricated dressings significantly reduce the inflammation and expedite wound healing *in vivo*.	Zhao *et al.*[89]
3	PUE/CA	Zn/AB	PUE-Zn/AB@CA dressing improves wound healing through the use of electrical stimulation and drug release. It shows strong antibacterial activity, especially against *E. coli* and *S. aureus*. Moreover, PUE impedes macrophage polarization to M1 both *in vitro* and *in vivo*, markedly diminishing pro-inflammatory cytokine expression in macrophages.	Chen *et al.*[90]
4	PCL/CA	CeO_2-CSNPs	CeO_2-CSNPs are effective at treating infections and oxidative stress in diabetic wounds due to their antibacterial, anti-oxidant, and anti-inflammatory properties. Electrospun nano-fibers facilitate cell attachment, nutrition transport, and moisture retention, which are necessary for healing. *In vivo* studies show that nanofibers can enhance the repair rate of diabetic wounds by 95.47% after 15 days.	Kamalipooya *et al.*[91]
5	PAN/PEO	Carvacrol	Carvacrol incorporated electrospun nanofibers prevent wound infections. Hydrophilic PEO improves moisture retention, which helps in maintaining an ideal wound environment. *In vivo* studies carried out on rats infected with *S. aureus* confirm the antibacterial nature and healing efficacy of the nanofiber membranes.	Wang *et al.*[92]
6	SA/PVA	Shikonin	Shikonin loaded nanofibers have good hydrophilicity, allow for suitable gas exchange, and keep the wound environment moist. These nanofibers exhibit good antibacterial and antioxidant nature. *In vivo* studies reveal a significant wound healing rate of 85.5% in diabetic mice.	Ding *et al.*[93]
7	PLGA/GL	Ciprofloxacin hydrochloride/quercetin	Ciprofloxacin hydrochloride and quercetin incorporated nanofibers with antibacterial and antioxidant features improve healing and show complete re-epithelialization within 16 days following the excision of full-thickness wounds *in vivo*.	Ajmal *et al.*[94]
8	Hyaluronic acid/ chitosan/PVA	Temporin-Ra peptide	Temporin-Ra adsorbed nanofibers have a high swelling ratio and they also enhance cell adhesion, proliferation, and migration. By promoting the inflammatory phase in shorter time, temporin-Ra speeds up wound healing and tissue repair. *In vivo* studies carried out on a murine model demonstrate 60% wound closure in the case of peptide-loaded nanofibers as compared to 17% wound closure in the control group.	Koohzad *et al.*[95]
9	Chitosan/silk fibroin	α-TCP/N-CQDs	Incorporation of α-TCP/N-CQDs in nanofibers enhances antibacterial efficiency resulting in lowered MIC values against *E. coli* and *S. aureus. In vivo* studies carried out on a rat model validate that the fabricated nanofiber can effectively enhance wound closure by 96.73 ± 1.25% within 12 days. Furthermore, histopathological analyses confirm expedited re-epithelization and a well-organized epidermis.	Dehghani *et al.*[96]
10	PVA/GL/PLGA	Thrombin and vancomycin	Nanofibers show antibacterial and antibiofilm activities against *S. aureus*. The scaffold's sustained drug release feature increases its therapeutic potential, while its good swelling index enables efficient absorption of wound exudates allowing for more rapid wound healing. *In vivo* studies carried out on a rat model demonstrate accelerated blood coagulation and faster wound closure.	Pandey *et al.*[97]

Table 1 *(Contd.)*

S. no.	Nanofiber material	Active component	Remarks	Ref.
11	GL/PCL	PDRN	The combination of PDRN with GL/PCL nanofibers produces a biomaterial with improved biocompatibility, collagen synthesis, and cell proliferation. *In vitro* drug release study shows 25% release over 7 days at pH 7.4 and 37 °C. *In vivo* results demonstrate that PDRN incorporated fibers exhibit markedly accelerated initial wound healing and closure relative to the control group after 3 and 4 weeks.	Kim *et al.*[98]
12	GL/graphene oxide	NAC	Combination of graphene oxide, GL, and NAC provides high mechanical strength, reactive oxygen species (ROS) scavenging behavior and a prolonged NAC release profile. Moreover, a higher burst release of NAC is observed in the first day followed by sustained release up to 14 days. *In vivo* studies reveal faster wound healing, reduced scar formation, and improved collagen regeneration in the case of NAC loaded nanofiber treated mice.	Yu *et al.*[99]
13	Chitosan/PEO	Cur@β-CD/AgNP	Combining Cur@β-CD/AgNP with nanofibers improves infection resistance against *P. aeruginosa*, *S. aureus* and *E. coli*. The higher water absorption capability of nanofibers helps in removing wound exudate and maintains a moist environment. *In vitro* drug release study shows that curcumin release from nanofibers is higher at pH 5.5 (≈72% release over 48 h) than at pH 7.4 (≈47% release in 48 h), owing to the destruction of ionic interactions at lower pH. *In vivo* studies display enhanced wound closure rates and less scar formation in comparison with commercial Aquacel Ag.	Liu *et al.*[100]
14	Chitosan/PEO	Kaolin	Incorporation of kaolin in nanofibers improves haemostatic performance and lowers blood clotting time (43 ± 1.4 s) as compared to bare nanofibers (61 ± 2.2 s) and QuikClot® Combat Gauze (55.7 ± 1.2 s). *In vivo* rat liver injury test also confirms enhanced hemostatic behavior. It also facilitates wound healing in rats within 14 days exhibiting minimal inflammatory response.	Liu *et al.*[101]
15	CA	Pramipexole	Pramipexole-loaded nanofibers exhibit antioxidant activity and a controlled drug release profile. The system shows ≈64% release in 24 h, finally reaching ≈96% release in 144 h. Moreover, *in vivo* studies on rats demonstrate that CA/3% pramipexole scaffolds display improved wound closure, epithelial thickness, and collagen deposition.	Tan *et al.*[102]
16	PVA/chitosan-g-PNVIM	TiO_2/curcumin	PVA/chitosan-g-PNVIM/TiO_2/curcumin nanofibers show antibacterial activity against *E. coli* and *S. aureus* with 90% growth inhibition in 1 h. *In vivo* studies performed on a rat model display enhanced wound closure in 14 days in the case of TiO_2/curcumin incorporated nanofibers as compared to control and unloaded nanofibers.	Motasadizadeh *et al.*[103]
17	Chitosan/PEO/collagen	Curcumin	Controlled release of curcumin from nanofibers over 3 days offers sustained anti-inflammatory, antioxidant, and antibacterial properties enhancing healing efficacy and diminishing infection risk. *In vivo* studies performed on rat models reveal accelerated wound closure relative to untreated wounds underscoring the efficiency of curcumin in wound healing.	Jirofti *et al.*[104]
18	PCL/chitosan	CURCSNPs	Electrospraying of CURCSNPs on curcumin incorporated PCL/chitosan nanofibers offers improved antibacterial, antioxidant, and cell proliferation abilities making it suitable for infected wounds. The *in vitro* cumulative drug release profile shows ≈22% release in the first 6 h, followed by a slow and sustained release of ≈49% over 3 days. *In vivo* studies reveal improved wound closure, particularly for methicillin-resistant *S. aureus* (MRSA)-infected mouse wounds.	Fahimirad *et al.*[105]
19	PCL/GL	*Gymnema sylvestre* extract/minocycline hydrochloride	These core–shell nanofibers, prepared for treating second degree burns, have minocycline hydrochloride loaded PCL/GL as a shell and *Gymnema sylvestre* extract loaded GL as the core. They exhibit antibacterial and antibiofilm efficacy against *S. aureus* and *P. aeruginosa*. *In vivo* studies reveal that nanofiber treated wounds exhibit enhanced re-epithelialization and collagen organization.	Ramalingam *et al.*[106]

Table 1 *(Contd.)*

S. no.	Nanofiber material	Active component	Remarks	Ref.
20	PCL/PVA/collagen	*Momordica charantia* pulp extract	Biological activity of *Momordica charantia* extract provides antioxidant, anti-inflammatory, and antibacterial activities to the nanofibers. This integration enhances healing outcomes as indicated by better wound closure rates and favourable histological results *in vivo*.	Salami *et al.*[107]
21	Chitosan/PEO/silica	Ciprofloxacin	Incorporation of silica improves collagen production and structural stability that promote wound healing. Here, the rapid initial release helps in eliminating infection, while the subsequent prolonged release maintains antibacterial activity over time. *In vivo* studies demonstrate that nanofibers greatly enhance wound healing by reducing inflammation in a mouse model.	Hashemikia *et al.*[108]
22	PCL/GL	Curcumin/surfactin	A bifunctional electrospun nanocomposite loaded with surfactin and curcumin facilitates healing and shows antibacterial activity especially against *S. aureus*. *In vivo* studies performed on Wistar rats confirm complete wound closure within 14 days.	Hadizadeh *et al.*[109]
23	Chitosan/GL	Cinnamon extract	Cinnamon extract-loaded electrospun nanofibers display antibacterial activity particularly against *S. aureus. In vitro* and *in vivo* results demonstrate that cinnamon concentration (25%) enhances antibacterial efficacy but it diminishes cell viability and impedes wound healing.	Ahmadi *et al.*[110]
24	Polygalacturonic/ hyaluronic acid	AgNPs	Incorporation of AgNPs in nanofibers significantly enhances antibacterial activity against *B. subtilis*, *S. aureus*, and *E. coli*. Nanofibers also have antioxidant and anti-inflammatory properties, which are important for reducing oxidative stress and speeding up wound healing. Furthermore, the study indicates that these nanofibers allow greater wound contraction and epithelialisation *in vivo*.	El-Aassar *et al.*[111]
25	Chitosan/SA	Gentamicin	Gentamicin loaded nanofibers show antibacterial activity against *E. coli* and *S. aureus*. *In vivo* experiments demonstrate that nanofibers loaded with 3% gentamicin markedly improve skin regeneration in a Balb/C mouse model. It promotes the development of a thicker dermis, collagen deposition, and formation of new blood vessels and hair follicles.	Bakhsheshi-Rad *et al.*[112]

molecular weight and viscosity) may lead to alterations in the physicochemical properties of the developed fibers.[55]

Furthermore, synthetic polymers such as polycaprolactone (PCL), poly(L-lactic acid) (PLLA), and poly(lactic-*co*-glycolic acid) (PLGA), as well as their copolymers, have also been extensively used for creating electrospun nanofibers due to their uniform physicochemical properties, tunable mechanical properties, predictable degradation rates, and ease of processing.[55–59] Electrospun PLGA nanofibers loaded with metformin have demonstrated sustained drug release, enhanced collagen deposition and reduced inflammation in diabetic and burn wounds.[6] Similarly, PLLA-based nanofibers have shown hemostatic potential and efficacy as drug carriers, further extending their application in wound care.[60,61]

In recent years, researchers have also combined both natural and synthetic polymers to obtain composite nanofibers with enhanced mechanical strength while maintaining bioactivity.[62–64] For instance, PCL nanofibers exhibit long-term stability in wound environments and are frequently blended with natural polymers like GL, chitosan, and collagen to improve bioactivity.[65–68] Blended electrospun fibers, such as poly(vinyl alcohol) (PVA)/sodium alginate (SA), chitosan/PVA, chitosan/GL/polyurethane, silk fibroin/PVA and PCL/GL are some other examples in this area exhibiting improved mechanical stability and bioactivity, thus making them ideal for wound healing applications.[45,65,69–74]

Moreover, incorporation of bioactive agents (*e.g.*, endothelial growth factor (EGF) and basic fibroblast growth factor (bFGF)) and nanomaterials has also helped in significantly enhancing the functionality of electrospun nanofibers.[75–77] For example, silver nanoparticle loaded PVA nanofibers exhibited antibacterial properties.[78] On the other hand, poly(hydroxybutyrate-*co*-hydroxyvalerate) (PHBV) nanofibers combined with modified keratin demonstrated effective diminution of scarring and preserved wound hydration.[79]

To adjust the physicochemical properties of electrospun nanofibers according to the requirements, advanced electrospinning techniques such as emulsion and co-axial electrospinning have gained attention in recent years.[80] These techniques allow for the fabrication of core–shell fibers capable of encapsulating drugs or growth factors in a unique manner, thus offering sustained release.[81,82] In this direction, Wang *et al.* utilized coaxial electrospinning to prepare polydopamine modified PCL/chitosan based core–shell nanofibers.[82] These nanofibers demonstrated excellent hydrophilicity, stretchability similar to human skin, and sustained release of EGF/bFGF.

Here, EGF/bFGF were encapsulated in the core and their release (≈45.98 and ≈40.43 for EGF and bFGF, respectively, in 3 days) was attributed to both degradation and diffusion mechanisms. It was observed that degradation-based release was dominant, which can be attributed to the encapsulation of the growth factor in the core of the nanofibers.

Furthermore, integration of stimuli-responsive materials into nanofibers provides the opportunity for developing multifunctional wound dressings.[83] Stimuli-responsive materials are designed to interact with endogenous stimuli (such as pH, reactive oxygen species (ROS), or enzymes) or exogenous stimuli (such as light, magnetic fields, or electrical signals) to enhance wound healing.[84] By responding to specific environmental triggers, stimuli-responsive materials can enhance therapeutic efficacy and optimize treatment outcomes.[84] For example, Gautam *et al.* developed smart thermal-responsive poly(*N*-isopropylacrylamide) (PNIPAM) and poly(methyl methacrylate) (PMMA) based electrospun nanofibers loaded with carbon quantum dots.[85] PNIPAM showed temperature responsive behavior due to its lower critical solution temperature (LCST) at ≈32 °C, thus undergoing a reversible hydrophilic-to-hydrophobic phase transition above this threshold. PMMA enhanced the structural stability of nanofibers and suppressed their premature dissolution in aqueous medium. The temperature-sensitive nature of PNIPAM enabled an on-demand release of the loaded carbon quantum dots (≈80%) upon temperature stimulation. It was reported that upon exposure to temperature above the LCST, PNIPAM segments collapsed, leading to increased porosity and expulsion of embedded carbon quantum dots, whereas cooling reversed this transition. Furthermore, Zhang *et al.* reported a multifunctional stimuli-responsive Janus electrospun nanofiber-based dressing.[86] It was fabricated to integrate drug release, wound pH monitoring, and unidirectional fluid drainage for enhanced wound healing. The Janus nanofiber was constructed using two electrospun layers: a hydrophobic PLLA based layer embedded with oxacillin and polyoxometalate, and a hydrophilic polyacrylonitrile (PAN) based layer loaded with phenol red to serve as a real-time pH sensor. A time-dependent drug release study showed that ≈60% polyoxometalate and ≈71% oxacillin were released within 24 h. Furthermore, the release of polyoxometalate in the first 3 h was faster than that of oxacillin, which was beneficial for antibacterial behavior. It was noted that the smart mats exhibited an obvious color change as the pH varied from 5.5 to 8.5, which is relevant to the wound physiological environment, demonstrating huge potential for wound monitoring. Notably, the phenol red loaded PAN layer maintained stable colorimetric performance at various temperatures (−20 °C to 40 °C) and could be reversibly reused for pH detection, confirming thermal stability and functionality.

Despite their numerous advantages, electrospun nanofibers face several challenges like scalability of the electrospinning process and insufficient mechanical strength that is often encountered.[87] Their naturally elevated surface area and porous composition, although advantageous for drug loading and cellular interaction, may result in dehydration of the wound bed.[6] This can restrict their capacity to sustain a moist healing environment.

The abbreviations used herein are as follows: HDIC: hydroxypropyl-β-cyclodextrin/dihydromyricetin inclusion complexes; PHL@CD: phloretin (PHL) encapsulated with γ-cyclodextrin (γ-CD); PUE: puerarin; CA: cellulose acetate; Zn/AB: zinc/acetylene black nanoparticles; CeO_2-CSNPs: chitosan nanoparticles encapsulated with green synthesized cerium oxide nanoparticles using *Thymus vulgaris* extract; PAN: polyacrylonitrile; PEO: poly-(ethylene oxide); α-TCP/N-CQDs: α-tricalcium phosphate/nitrogen-doped carbon quantum dot nanocomposite; PDRN: starfish polydeoxyribonucleotides; NAC: *N*-acetyl cysteine; Cur@β-CD/AgNP: β-cyclodextrin stabilized silver and curcumin based nanoparticles; PNVIM: poly *N*-vinyl imidazole; TiO_2: titanium dioxide; CURCSNPs: curcumin-loaded chitosan nanoparticles; and AgNPs: silver nanoparticles.

5. Functional hydrogels

Hydrogels are three-dimensional, cross-linked networks of polymers that can absorb significant amounts of water.[113] They play a critical role in maintaining a moist environment, which is essential for accelerated wound healing. They are typically applied as the inner contact surface with the wound bed, providing multiple functions such as exudate absorption, adhesiveness, localized drug delivery, hemostasis, anti-inflammatory, antibacterial, and self-healing properties.[114–116] They also display stimuli-responsive behavior making them a suitable alternative for wound treatment.[117] These are made up of either natural or synthetic polymers, each presenting its own unique features.[113] Natural polymer based hydrogels derived from chitosan, alginate, and GL exhibit biodegradability and bioactivity. However, they are deficient in mechanical strength and uniformity of the polymer batches.[118,119] On the other hand, synthetic polymer (*e.g.*, PVA, PEG, and acrylamide) based hydrogels exhibit better mechanical properties and tunability. However, they often lack required biocompatibility and biodegradability.[119] Some recent examples of hydrogels highlighting their characteristic features and *in vivo* implications are summarized in Table 2.

The adhesive properties of hydrogels play an important role in closely adhering it to the underlying tissue, thereby minimizing scarring. This helps in substituting traditional methods such as the use of sutures.[120] In this direction, Ma *et al.* developed SA, calcium ions (Ca^{2+}), acrylamide, acrylated guanine, and acrylated dopamine based hydrogels featuring triple-crosslinking networks.[121] This hydrogel provided self-healing properties, electrical conductivity, and biocompatibility, exhibiting superior adhesion and mechanical strength. Chen *et al.* synthesized gelatin methacrylate, adenine acrylate, and $CuCl_2$ based hydrogels employing covalent bonding, coordination complexation, and hydrogen bonding.[122] These hydrogels exhibited a self-healing feature, fatigue resistance, and adhesive properties offered by hydrogen bonds and

Table 2 Recent advances in functional hydrogels for enhanced wound healing and their *in vivo* implications

S. no.	Hydrogel material	Gel mechanism	Active component	Remarks	Ref.
1	Dopamine-grafted oxidized SA/GL	Dual cross-linking using Schiff base bonds and hydrogen bonds	MC@ZIF-8	The fabricated hydrogel shows good mechanical strength, adhesion, antioxidant and self-healing behavior. *In vivo* studies reveal that the MC@ZIF-8 loaded hydrogel improves wound healing by augmenting the expression of CD31 and COL1A.	Nezhad-Mokhtari *et al.*[147]
2	Chia seed mucilage	Electrostatic interactions	ZnO-NP/allantoin	ZnO-NP and allantoin loaded hydrogels show high biocompatibility, strong antibacterial activity, and significant reduction in wound size (90.7%) *in vivo* within 14 days.	Mahajan *et al.*[148]
3	Cellulose/chitosan	Schiff base	Eugenol	Eugenol-loaded hydrogels exhibit potent antibacterial activity through disruption of bacterial membranes by eugenol, leading to cell lysis. Additionally, the cationic nature of chitosan further enhances membrane destabilization, effectively inhibiting *S. aureus* and *E. coli*. Angiogenic potential is attributed to eugenol-induced upregulation of VEGF expression, promoting endothelial activation and neovascularization, as confirmed by gene expression analysis.	Khadim *et al.*[149]
4	PVA/aloe vera	Hydrogen bonding	Caffeine/vitamin C	Caffeine and vitamin C loaded hydrogels accelerate wound healing by enhancing fibroblast migration, collagen synthesis, and angiogenesis. Caffeine stimulates tissue regeneration *via* adenosine receptor blockade, while vitamin C promotes collagen formation and reduces oxidative stress. Aloe vera supports hydration and anti-inflammatory action. *In vivo* studies reveal that the hydrogels improve re-epithelialization, granulation, and wound contraction, leading to rapid and effective skin repair.	Kenawy *et al.*[150]
5	Alginate dialdehyde/ chitosan	Schiff base	Curcumin-loaded bilosomes	The fabricated hydrogel shows high water absorption and sustained drug release behavior. *In vivo* studies carried out on male albino rats reveal complete wound closure in three-weeks.	Sideek *et al.*[151]
6	Gelatin methacryloyl	Photopolymerization	LGG	The scaffold has good mechanical and self-healing properties. *In vivo* studies reveal that LGG loaded hydrogels inhibit bacterial infections and reduce proinflammatory cytokines by modulating the NF-κB and MAPK pathway. Simultaneously, reduced TGF-β and VEGFR2 expression limits excessive fibrotic response and aberrant angiogenesis, promoting balanced vascular remodeling.	Han *et al.*[152]
7	Silk fibroin/soy protein isolate	ECH cross-linking	Quercetin	Quercetin incorporated hydrogels have antioxidant and antibacterial properties. *In vivo* studies reveal that the hydrogels show epidermal regeneration, collagen deposition, and improved angiogenesis demonstrating superior wound closure.	Li *et al.*[153]
8	ADPM2S2	Cross-linking using strontium ions	Insulin	Insulin-loaded ADPM2S2 hydrogel promotes wound healing in diabetic wounds by regulating insulin release, thereby accelerating tissue repair. The system shows 40% release at pH 5.4, while 90% release was observed at pH 7.4 over 48 h. The release occurred following the Korsemeyer–Peppas model, and the α helical structure of the insulin molecule was maintained even after release. *In vivo* studies on diabetic rats reveal 95% wound closure in 14 days as compared to 82% in the control.	Rajalekshmy *et al.*[154]
9	Chitosan/collagen	Genipin crosslinking	cef.Na-AgNPs	cef.Na-AgNP loaded hydrogel functions as a structural framework with antibacterial activity against both Gram-positive and Gram-negative bacteria. *In vivo* studies reveal 98% wound closure in injured rats after two weeks.	Abdel-Gawad *et al.*[155]
10	Silk fibroin	Sol–gel mechanism	Vancomycin	Vancomycin loaded hydrogel has good biocompatibility and sustained drug release behavior. *In vivo* studies reveal a diabetic wound healing rate of 86.6%, thus outperforming the unloaded hydrogel (33.3%) and povidone (16.6%).	Singh *et al.*[156]
11	CMC/aldehyde-modified glycyrrhizic acid	Schiff base	Glycyrrhizic acid	Glycyrrhizic acid based hydrogel is a self-healing, injectable hydrogel with an intrinsic antibacterial property. *In vivo* studies reveal the healing ability of *S. aureus* infected full-thickness wounds by increasing granulation tissue formation, collagen deposition, and downregulating inflammation.	Li *et al.*[157]
12	PVA/GL	Cross-linking with tannic acid	Curcumin	The presence of tannic acid and curcumin in the system provides antioxidant and antibacterial behavior. Release study of curcumin shows an initial burst release of 40% in 6 h, followed by sustained release over 72 h. *In vivo* studies on a rat wound model reveal that the loaded hydrogel shows 93% wound closure in 10 days which outperforms Cur cream and PG9.	Rashid *et al.*[158]

Table 2 *(Contd.)*

S. no.	Hydrogel material	Gel mechanism	Active component	Remarks	Ref.
13.	CMCs/oxidized hyaluronic acid	Imine bonds/electrostatic interactions	MPDA@Cur NPs/ metformin	The fabricated hydrogel has antibacterial, antioxidant, and anti-inflammatory properties. In a diabetic full-thickness wound in a rat model, the remaining wound areas after 14 days are: 20.9% for the control group, 15.9% for 3M Tegaderm™, 9.6% for the unloaded hydrogel, and 3.3% for the loaded hydrogel.	Tan *et al.*[159]
14	Dextran/gallic acid-grafted GL	Schiff-base/metal coordination	Gallic acid/ferric ions	This multifunctional hydrogel, having dynamic Schiff-base bonds and Fe^{3+}-mediated coordination with polyphenol/carboxyl groups, provides injectability, self-healing ability, and adhesion. Upon NIR irradiation, Fe^{3+}/polyphenol complexes generate a rapid photothermal effect, against both *E. coli* and *S. aureus*. Gallic acid moieties in the hydrogel scavenge excess ROS, reducing oxidative stress and inflammation. The hydrogel also promotes hemostasis and angiogenesis, leading to complete re-epithelialization of infected diabetic wound in mice within 18 days.	He *et al.*[160]
15	SA/Pluronic F-127/PVA	Physical crosslinking	Naringenin	Addition of naringenin in hydrogels provides antioxidant, anti-inflammatory, and antibacterial properties. An initial burst release of 45.5% is observed in 6 h due to high drug loading and rapid swelling, followed by slower release reaching 83.2% in 12 h. *In vivo* studies show improved wound closure, re-epithelialization, and collagen accumulation in diabetic Wistar rats.	Raina *et al.*[161]
16	Silk fibroin/graphene oxide	EDC-NHS crosslinking	Ciprofloxacin	The fabricated hydrogel provides sustained drug release, while its structural integrity and porosity ensure oxygen permeability for cell proliferation and tissue regeneration. A cumulative release of ≈98% is achieved over 4 days. Here, initial burst release is due to rapid dissolution of the surface-bound drug, while sustained release results from the interplay of controlled degradation of the silk fibroin matrix and strong interactions between the drug and graphene oxide. *In vivo* burn wound studies reveal that it increases wound contraction, collagen deposition, granulation tissue thickness, and vascularization.	Dong *et al.*[162]
17	Dialdehyde starch/GL	Schiff base	MBGNs	The fabricated hydrogel has high adhesive strength and self-healing properties. MBGNs release Si^{4+} and Ca^{2+} ions which stimulate angiogenesis and fibroblast proliferation. *In vivo* studies also reveal improved haemostasis and faster skin wound healing than surgical closures.	Tian *et al.*[163]
18	Collagen/hyaluronic acid	EDC-NHS crosslinking	EGF	The scaffold has excellent biocompatibility and strong antioxidant properties. *In vitro* release profile reveals initial burst release of EGF followed by sustained release up to 20 days, which improves cell proliferation and reduces inflammation. Moreover, histological analysis reveals re-epithelialization, granulation tissue formation, and tissue remodelling in the case of the loaded hydrogel.	Wang *et al.*[164]
19	Hyaluronic acid/poly (ethylene glycol)-*co*-poly (glycerol sebacate)	Schiff base	CMP	The hydrogel has excellent self-healing ability, injectability, strong tissue adhesion, antioxidant properties, and photothermal antibacterial property for infection control. *In vivo* studies reveal its efficacy in promoting healing for full-thickness skin wounds by inhibiting infection, fastening collagen deposition, and increasing granulation tissue formation.	Li *et al.*[165]
20	GL/PVA/siloxane network	Sol–gel crosslinking	Si-CAQ	The dressing is effective against bacteria (such as *E. coli*and *B. subtilis*) for a longer period of time. *In vivo* studies indicate that it promotes wound healing by enhancing re-epithelialization, collagen maturation, and vascularization.	Gharibi *et al.*[166]
21	L-DOPA and ε-poly-L-lysine modified hydroxybutyl chitosan	Phenol cross-linking	BMSCs	This hydrogel has several benefits including strong wet tissue adhesion and antibacterial activity owing to the presence of L-DOPA and ε-poly-L-lysine, respectively. Furthermore, the encapsulated BMSCs produce growth factors and cytokines to enhance fibroblast migration and collagen deposition, improving wound healing *in vivo*.	Tian *et al.*[167]
22	SA/GL	Electrostatic interactions	AgNPs	AgNP-loaded hydrogels are biocompatible, promote cell adhesion, and have antibacterial properties. *In vivo* studies on female Wistar rats reveal a significant decrease in wound size with earlier granulation tissue development and maturation.	Diniz *et al.*[168]

Table 2 *(Contd.)*

S. no.	Hydrogel material	Gel mechanism	Active component	Remarks	Ref.
23	Quaternized chitosan/ phosphorylated chitosan	Electrostatic and van der Waals interactions	Tannic acid and poly-ε-lysine	The fabricated hydrogel has a high absorption rate and strong adhesive property. It shows good haemostatic behavior. *In vivo* studies on Wistar rats demonstrate that the fabricated hydrogel is non-toxic and biocompatible.	Singh *et al.*[169]
24	Oxidized *Bletilla striata* polysaccharide/chitosan	Schiff-base	*Lactobacillus plantarum* probiotic	The composite probiotic hydrogel is biocompatible and has antibacterial properties against *S. aureus*, *E. coli*, and *P. aeruginosa*. *In vivo* studies using a full-thickness skin defect model show excellent wound healing efficacy.	Yang *et al.*[170]
25	Hyaluronic acid modified with alkylamines	Carbodiimide crosslinking	Nitric oxide	The nitric oxide-releasing hydrogel combines antibacterial and wound healing properties, offering broad-spectrum protection against drug-resistant and biofilm-based infections. In infected murine wounds, it offers accelerated wound closure while reducing the *P. aeruginosa* genetic material in the remaining tissue.	Maloney *et al.*[171]

metal–ligand coordination. Release studies revealed the burst release of Cu^{2+} in the first 5 days followed by sustained release over 5–7 days. Initial release provided antibacterial behavior to the hydrogel while subsequent slow release promoted angiogenesis.

Furthermore, chronic wounds frequently exhibit excessive inflammation which obstructs the healing process.[115] Anti-inflammatory hydrogels regulate macrophage polarization, eliminate ROS, and sequester pro-inflammatory chemokines.[115] To address the issue of inflammation, Zhao *et al.* developed a hydrogel utilizing biocompatible polymers and conductive polyaniline-based derivatives.[123] This hydrogel was loaded with polydopamine-modified natural catalase mimicking nanozyme to reduce ROS and regulate the immune response, thereby accelerating the closure of diabetic foot ulcers. In this direction, Chen *et al.* developed a H_2S-releasing multifunctional hydrogel utilizing the dynamic Schiff base reaction between carboxymethyl chitosan (CMCs) and polyhexamethylene guanidine-modified aldehyde F108 (PFC).[124] Diallyl trisulfide (DATS) loaded in the developed system released H_2S slowly in the presence of glutathione, exerting anti-inflammatory effects by inhibiting the expression of p-ERK and pSTAT3 in activated macrophages, and promoting macrophage polarization to the M2 phenotype.

A major concern in the wound healing process is bacterial infection that extends the inflammatory phase, impeding wound healing. Prolonged inflammation leads to excessive exudate production and tissue damage, which may result in sepsis or death.[125] Hence, hydrogel based wound dressings are endowed with antibacterial properties to mitigate these concerns. Cheng *et al.* prepared a cationic hydrogel *via* chemical crosslinking of *trans*-1,4-cyclohexanediamine with 1,3-dibromo-2-propanol.[126] This method yielded a hydrogel exhibiting robust antibacterial efficacy against *S. aureus* and *E. coli*. Yang *et al.* developed a multifunctional hydrogel composed of polyethylene glycol monomethyl ether modified glycidyl methacrylate functionalized chitosan, methacrylamide dopamine, and zinc ions that effectively inhibited methicillin-resistant *S. aureus*.[127] The hydrogel showed a burst release of zinc ions (62.5 μg mL^{-1}) within 1 h and a sustained release (118.8 μg mL^{-1}) up to 288 h that provided a long-term antibacterial property to the hydrogel. Cheng *et al.* developed a sprayable catechol modified gelatin methacryloyl hydrogel incorporated with the antibacterial peptide HHC-36 and cerium oxide nanoparticles.[128] The reported hydrogel showed a combination of antibacterial and ROS scavenging capabilities. Additionally, the release of HHC-36 from the hydrogel showed rapid release ablation and contact ablation against four bacterial strains, confirming antibacterial activity.

The antioxidant activity in a hydrogel is also very important as it helps in addressing oxidative stress which is a key factor responsible for impaired wound healing.[129] To address this, Qi *et al.* developed a cationic guar gum based hydrogel loaded with tannic acid based microsized particles.[130] The prepared hydrogels showed antioxidant behavior and photothermal characteristics which were augmented by NIR light. Wang *et al.* developed a lipoic acid-modified chitosan hydrogel *via* amidation reaction. Furthermore, ceria oxide-molybdenum disulfide nanoparticles coated with a polydopamine layer, and carbon quantum dots synthesized by a hydrothermal method were loaded into the hydrogel.[131] The fabricated hydrogel exhibited excellent photothermal antibacterial activity against *S. aureus* and *E. coli*. The remarkable antioxidant and anti-inflammatory abilities of the hydrogel facilitated alleviation of ROS and relief from inflammatory responses during wound healing.

Furthermore, the hemostatic properties in the hydrogel can expedite recovery by enhancing coagulation factors and platelets to facilitate clot formation.[132] In this regard, Tan *et al.* developed a composite hydrogel dressing through free radical polymerization of methacrylate gelatin, bisphosphonic acid and cyclodextrin-modified hyaluronic acid.[133] The hydrogel was loaded with the anti-inflammatory drug resveratrol through supramolecular inclusion. The fabricated hydrogel exhibited burst release of resveratrol in the first two days, which helped to promote anti-inflammation. Further sustained release of resveratrol was observed up to 14 days. After implantation into bleeding wounds, the hydrogel electro-

statically enriched blood cells and platelets around the wound area to accelerate thrombosis and also increased its own weight to compress local blood vessels for reducing blood loss. In another study, Kamedani *et al.* fabricated an injectable and hemostatic hydrogel utilizing carbohydrazide-modified GL and monoaldehyde-modified hyaluronic acid.[134] *In vivo* studies carried out in mouse models showed that the hemostatic capability of hydrogels was comparable to that of fibrin glue.

Furthermore, self-healing hydrogels are gaining significant attention as they can recover from mechanical damage. These hydrogels can restore their structure and therapeutic efficacy even after damage by using reversible dynamic linkages.[135] For example, Huang *et al.* reported a Schiff base crosslinked quaternized chitosan/oxidized dextran based self-healing hydrogel.[136] It was loaded with tobramycin (TOB) and polydopamine-coated polypyrrole nanowires (PPY@PDA). The acidic substances generated in the process of bacterial growth offered pH-responsive release of TOB due to the degradation of Schiff base units, thus protecting wound from infection. Furthermore, the incorporation of PPY@PDA in the hydrogel provided near-infrared irradiation assisted bactericidal activity against drug-resistant bacteria, conductivity, and antioxidant activity. Cao *et al.* fabricated a CMC based injectable self-healing hydrogel utilizing trivalent metal ions of Fe^{3+} and Al^{3+} to form coordination bonds with CMCs.[137] The fabricated hydrogel exhibited self-healing behavior owing to the dynamic and reversible characteristics of the coordination bonds. Furthermore, recent advances have shown the significance of self-healing hydrogels in tissue engineering, particularly for load-bearing and dynamic environments like cartilage and muscle. Thomas *et al.* developed a peptide–polysaccharide double-network hydrogel using amyloid-inspired peptide amphiphile based nanofibers and a dynamic polysaccharide matrix formed *via* Schiff base crosslinking between carboxymethyl cellulose dialdehyde and carboxymethyl chitosan.[138] The hydrogel exhibited self-healing, injectability, and enhanced mechanical strength suitable for cartilage repair. The incorporation of peptide based nanofibers significantly improved energy dissipation, pore structure, and mechanical recovery while also promoting chondrocyte adhesion, proliferation, and extracellular matrix production *in vitro*. Similarly, Nath *et al.* reported a self-healing hydrogel by tweaking the nanoscale structures of the peptide amphiphile from nanofibers to twisted bundles that were further crosslinked with an aldehyde-functionalized polymer using dynamic Schiff base chemistry.[139] The conjugated hydrogel showed increased load-bearing capacity, compressibility, and fibroblast and myoblast proliferation, and facilitated the formation of multinucleated myotubes, thus offering great promise in muscle tissue engineering. In another study, Joseph *et al.* demonstrated the formation of a peptide–PNIPAM copolymer based self-healing hybrid hydrogel utilizing pH responsive Schiff base crosslinking.[140] The fabricated hydrogel was biocompatible for U2OS cell lines and provided ideal mechanical cues for enhanced cell proliferation with potential for muscle actuation. Additionally, Chandran *et al.* reported a Fe(II)-guanosine-5′-monophosphate/tetra(4-carboxylphenyl) ethylene based supramolecular hydrogel.[141] The incorporation of ferrous ions enhanced the storage modulus, reinforcing the hydrogel's mechanical integrity. It also enabled reversible gel–sol transitions and 94% recovery in thixotropic tests, confirming its self-healing behavior. These properties are crucial for dynamic tissue environments such as bone and cartilage, where mechanical cues and self-repair capacity support cell proliferation and matrix remodeling. Moreover, the hydrogel's Fenton reaction-mediated ROS generation, particularly when boosted with ascorbic acid, facilitated broad-spectrum antimicrobial activity against Gram-positive, Gram-negative, and drug-resistant bacterial strains, supporting its potential utility in infected bone or cartilage regeneration.

In recent years, increasing focus has been given to design hydrogels with stimuli-responsive features. These hydrogels can alter their structure and physicochemical or mechanical properties in response to external stimuli. Such smart hydrogels, responsive to temperature, pH, light, pressure, and ionic fluctuations, are being examined for their potential in treating wounds.[117] It is to be noted that in diabetic wounds, increased MMP9 levels are associated with inadequate healing. To address this issue, Lin *et al.* developed an MMP-9 responsive injectable hydrogel utilizing oxidized hyaluronic acid and hydrazide grafted gelatin.[142] It was loaded with the drug cinnamaldehyde. In the presence of MMP-9, gelatin was degraded and cinnamaldehyde was continuously released in an inflammation-responsive manner. This inhibited the ferroptosis of traumatic endothelial cells and accelerated the healing of diabetic wounds. Furthermore, Liang *et al.* developed a metformin loaded dual responsive hydrogel utilizing Schiff base linkages sensitive to pH and phenylboronate ester linkages sensitive to glucose.[143] It was observed that metformin release was 30.4% higher at pH 5.5 than at pH 7.4, and 12.7% higher at pH 6.8 than at pH 7.4. This could be attributed to the dissociation of Schiff base linkages under acidic conditions. Additionally, for diabetic wounds, prolonged inflammation often leads to lower pH which can help in metformin release at the wound site. The system also possessed self-healing and tissue adhesive characteristics, which maintained the integrity of the wound dressing. Sharma *et al.* reported a hydrogel integrating a piezo-driven triboelectric nanogenerator to deliver self-generated electrical stimulation (ES) to wounds.[144] This interactive dressing mimicked skin-like properties, offering both electrical cues and a moist wound environment essential for healing. The ES generated by biomechanical activity significantly enhanced fibroblast proliferation and endothelial cell alignment, leading to accelerated re-epithelialization, neovascularization, and overall tissue remodeling in a full-thickness wound model. Readers are further recommended to refer to several review articles for detailed information on various aspects of stimuli responsive hydrogels for wound healing.[10,84,145,146]

In actual medical scenarios, wounds are generally classified into two major categories: acute and chronic wounds. Acute wounds typically result from surgical procedures or trauma,

and progress through the normal healing phases without complications.[24] On the other hand, chronic wounds such as diabetic foot ulcers or pressure sores often become stalled in the inflammatory phase, requiring more advanced and prolonged care strategies.[24] To effectively address these wounds, hydrogels must exhibit a range of functional properties. For acute wounds, adhesion, moisture retention, and hemostatic capability are critical to ensure rapid closure and protection.[145] In contrast to acute wounds, chronic wounds demand hydrogels with more advanced functionalities, such as antibacterial, antioxidant, and anti-inflammatory properties to prevent infection, oxidative stress, and inflammation.[145] While hydrogels have been engineered to possess these properties mentioned above, challenges remain in their clinical translation. Wound healing is a complex, multistage process where each stage demands a specific microenvironment and biological support.[146] Hence, the key challenge lies in designing smart hydrogels that can adapt dynamically to the evolving needs of the wound over time, ultimately supporting each phase of healing in a timely and targeted manner. Additionally, adhesive hydrogel patches, which can be applied on the wounds, should be designed with the feature of easy removal on demand. Furthermore, incorporation of the wound monitoring feature in hydrogels can help in better wound care in future. This should also be aligned with the adjustment of the release of bioactive components according to the requirement of the wound site as judged by the dynamic monitoring data.

The abbreviations used herein are as follows: MC@ZIF-8: *Myrtus communis* L. extract incorporated into a zeolitic imidazolate framework; ZnO-NP: zinc oxide nanoparticles; LGG: *Lacticaseibacillus rhamnosus*; GG; ECH: epichlorohydrin; ADPM2S2: alginate conjugated with diamine poly(ethylene glycol) molecules, followed by grafting with poly(ethylene glycol) methacrylate; cef.Na-AgNPs: cefotaxime sodium-loaded silver nanoparticles; CMCs: carboxymethyl chitosan; MPDA@Cur NPs: curcumin, loaded mesoporous polydopamine nanoparticles; EDC: 1-(3-dimethylaminopropyl)-3-ethylcarbodiimide hydrochloride; NHS: *N*-hydroxysulfosuccinimide sodium salt; MBGNs: mesoporous bioactive glass nanoparticles; CMP: cuttlefish melanin nanoparticles; Si-CAQ: silanized quaternary ammonium salt based on castor oil; L-DOPA: L-3, 4-dihydrox-yphenylalanine; and BMSCs: bone marrow mesenchymal stem cells.

6. Bilayer dressings

Bilayer dressings help mimic the physiology and functions of natural skin while providing a supportive platform for cellular migration and proliferation.[14] The concept of bilayer dressings is impelled by the structural organization of skin having the epidermis and dermis. Bilayer dressings are formed by leveraging the combination of electrospun nanofibers and hydrogels.[172–174] Here, the hydrogel layer provides an ideal microenvironment for cellular attachment and proliferation while exhibiting anti-inflammatory behavior. Its porous structure allows for optimal exchange of nutrients and gases at the wound site which is required for efficient wound healing.[175–177] On the other hand, the nanofibrous layer acts as a structural and protective layer. It provides external coverage to the hydrogel, safeguarding the wound from environmental contaminants.[178] Additionally, the nanofibrous layer acts as a physical barrier against the bacterial invasion, thus minimizing the risk of wound infections.[44,172] The material design requirements for a bilayer wound dressing necessitate a balance of structural, mechanical, and functional properties to promote enhanced wound healing. A critical aspect of such designs is ensuring robust interfacial adhesion among monolayer counterparts to prevent delamination during handling or application, which could otherwise compromise the dressing's protective and therapeutic efficacy.[179] To achieve effective adhesion, various strategies have been employed, including surface modification, chemical crosslinking between layers, formation of interpenetrating networks at the interface, and a low-pressure filtration-assisted method, which help integrate the layers by facilitating uniform contact and partial entanglement or interdiffusion during fabrication.[174,180–182] In addition to interfacial adhesion, mechanical compatibility between the layers is essential, and a significant mismatch in stiffness between the layers can lead to mechanical failure and discomfort during application.[179] Moreover, to enhance the efficiency of bilayer dressings, various active features (*e.g.*, antibacterial, anti-inflammatory, and pro-angiogenic) are incorporated.[183,184] These active features can be incorporated either by the functionalization of polymers or by loading the layers with active components such as antibacterial peptides, growth factors, and other therapeutic agents.[173,183,185]

The recent advancement in bilayer dressings has focused on fast coagulation, exudate absorption, antibacterial activity, and enhanced tissue regeneration.[14,44,186,187] In this regard, Xia *et al.* reported bilayer artificial skin (PLLA-PA@Ga-CMCs/GL) (Fig. 2a).[14] It was assembled with a top nanofibrous layer and bottom hydrogel porous layer as shown in the scanning electron microscopy (SEM) image (Fig. 2b). Here, nanofibers were directly electrospun onto the freeze dried hydrogel layer to prepare the bilayer dressing. The dermis-mimicking layer was prepared with CMCs and GL gel network cross-linked with protocatechuic aldehyde (PA) and gallium ions (Ga^{3+}). This layer showed adjustable pore sizes (78–138 μm) and high porosity (75–90%) providing good air and moisture permeability (1535%) to allow gas exchange and promote cell migration and proliferation. Additionally, it demonstrated exceptional fluid absorption capabilities (2023% swelling rate and 1138% blood absorption) making it effective for maintaining a moist environment and absorbing wound exudates. It showed fast hemostatic performance evidenced by a clotting time of 67 s. It also exhibited a 99.9% bacterial inhibition rate displaying its potential for minimizing the risk of infection. The epidermis-mimicking layer, composed of electrospun PLLA nanofibers, provided a protective barrier against bacterial invasion and fluid loss while maintaining breathability. Overall, the efficacy of this bilayer artificial skin was demonstrated *in vivo* using a

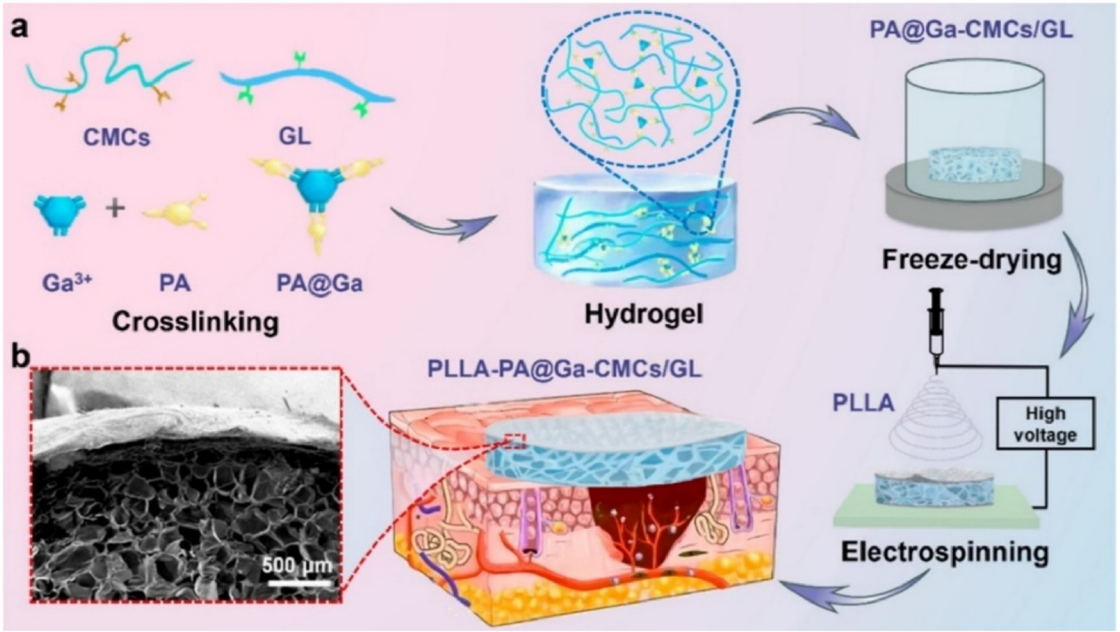

Fig. 2 (a) Schematic representation of the fabrication of PLLA-PA@Ga-CMCs/GL artificial skin and (b) cross-sectional SEM image of PLLA-PA@Ga-CMCs/GL. Adapted with permission from[14] Xia *et al.* Copyright 2024, American Chemical Society.

rat wound model. An *in vivo* study revealed that it accelerated wound closure and reduced inflammation. Furthermore, it also enhanced the formation of hair follicles and blood vessels, which is indicative of its efficacy to support skin regeneration.

Similarly, Mirhaj *et al.* developed a bilayer dressing by direct electrospinning of chitosan/L-arginine based electrospun nanofibers onto chitosan/polyethylene glycol based sponge enriched with advanced platelet-rich fibrin.[186] Release studies revealed that PDGF-AB and VEGF exhibited a sustained and gradually increasing release over a period of 7 days, which can be attributed to enhanced water uptake and swelling of the dressings over time. Moreover, the slow and sustained release of L-arginine from the dressing was attributed to chemical interactions between chitosan and L-arginine. This prolonged release offers therapeutic advantages by maintaining a stable effect at the wound site while minimizing the risk of toxicity associated with elevated concentrations. It also exhibited significantly higher antibacterial activity and angiogenic potential, and promoted cell viability and attachment of L929 fibroblasts. *In vivo* studies further validated its efficacy demonstrating accelerated wound closure and enhanced healing in full-thickness wounds in 12 days. Furthermore, Khan *et al.* also fabricated a bilayer dressing by direct electrospinning of PVA/bacterial cellulose nanofibers over a highly porous Ag-sulfadiazine loaded GL/PVA based freeze-dried hydrogel.[187] It exhibited high swelling capacity, degradability, and sufficient porosity. Additionally, it showed sustained release of Ag-sulfadiazine resulting in significant antibacterial activity against *E. coli*, *P. aeruginosa*, *and S. aureus*. *In vitro* studies using fibroblast and human embryonic kidney cells showed its excellent hemocompatibility, cell adhesion, viability, and proliferation.

Based on a similar approach of direct electrospinning, Cao *et al.* developed a bilayer dressing designed to accelerate chronic wound healing through its multifunctional properties.[44] In this system, the outer layer consisted of tetracycline hydrochloride (TH)-loaded PCL nanofibers. It acted as a protective barrier, offered antibacterial activity, and provided mechanical support for skin's natural movements. Furthermore, the ECM mimicking inner layer was composed of a PVA hydrogel incorporated with SA microspheres loaded with curcumin. The fabricated dressing enabled controlled release of TH and curcumin. 95% TH was released in 10 h, providing early antibacterial action. Curcumin showed pH-responsive release with the highest release under alkaline conditions (≈78% at pH 8.5 in 120 h), which is typically found in chronic wounds. The fabricated dressing also exhibited good antioxidant properties. Moreover, *in vivo* studies on a chronic diabetic wound model revealed the dressing's ability to significantly accelerating wound closure.

Similarly, Tavakoli *et al.* developed a bilayer wound dressing by integrating a hydrophilic sponge with electrospun nanofibers *via* direct electrospinning.[188] The sponge layer was composed of poly(acrylic acid) and honey. The average pore size of the sponge was 76 μm and it showed excellent water absorption capacity. The electrospun nanofibrous layer was composed of keratin, honey, and VEGF, facilitating sustained VEGF release over 7 days. This gradual release helped enhance angiogenesis as suggested by both *in vitro* and *in vivo* studies. Overall, the dressing demonstrated cytocompatibility with human keratinocyte cells and promoted cell attachment and

migration, thus accelerating tissue regeneration. It also showed enhanced blood vessel formation, collagen synthesis, and epidermal layer generation in animal models. Furthermore, Ramanathan *et al.* developed a bilayer matrix by combining electrospinning and freeze-drying techniques.[7] This bilayer dressing consisted of a CA based nanofibrous layer loaded with bioactive latex (L) or ciprofloxacin (D), and a spongy collagen matrix. An *in vitro* drug release study demonstrated an initial burst release of L (≈19%) and D (≈18%), followed by sustained release in the range of 75–85% over 72 h. Kinetic analysis indicated that the release followed zero-order and first-order models, with sustained release behavior best described by the Higuchi model. Mechanistically, L followed non-Fickian diffusion, while D exhibited Fickian diffusion, enabling effective infection control and promoting wound healing. The fabricated dressing showed high porosity, excellent swelling capacity, and stability required for efficient wound healing. It also supported the adhesion and proliferation of NIH 3T3 fibroblasts and HaCaT keratinocyte cells. Moreover, the nanofibrous layer showed better cell adhesion and proliferation as compared to the spongy layer of the bilayer matrix (Fig. 3). Additionally, the loading of L offered an antibacterial feature to the matrix against *S. aureus* and *P. aeruginosa*.

Recently, Han *et al.* developed hydrogen sulfide-releasing bilayer dressing by direct electrospinning of nanofibers on hydrogels.[172] This dressing was made up of a GL-based hydrogel layer and a polyurethane based electrospun nanofibrous layer. Here, the hydrogel layer contained a bio-macromolecular H_2S donor synthesized from a keratin–tannic acid conjugate. This layer facilitated fast absorption of wound exudates while acting as a reservoir for self-catalytic and sustained H_2S release. It promoted cell proliferation and migration, while providing antioxidant and ROS scavenging activities. Moreover, a polyurethane electrospun nanofibrous mat was embedded with glutathione, thus mimicking the epidermal layer by offering mechanical support, protection against bacterial invasion, and initiating H_2S release *via* a glutathione-triggered mechanism. The efficacy of this bilayer dressing was demonstrated utilizing a full-thickness wound model in rats. It was observed that the reported dressing significantly improved granulation tissue formation, collagen deposition, and vascularization, while also reducing inflammation and facilitating hair follicle regeneration.

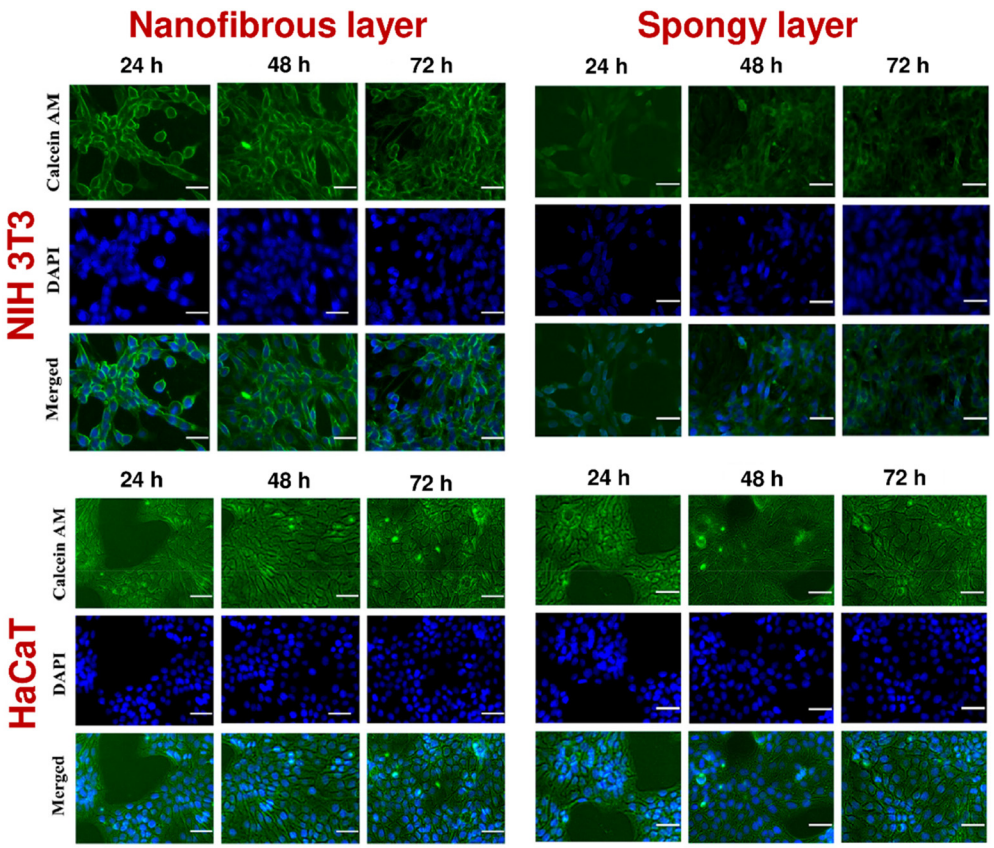

Fig. 3 Cell adherence and proliferation of NIH 3T3 fibroblasts and HaCaT keratinocytes on the nanofibrous layer and spongy layer of the bilayer matrix at 24, 48, and 72 h (scale bar = 100 μm). Adapted from[7] Ramanathan *et al.* Licensed under CC BY 4.0. View license: https://creativecommons.org/licenses/by/4.0/. Changes include replacing 'hour' with 'h', combining two figures, removing sub-labels (a and b), and adding annotations for the cell line name, nanofibrous layer, and spongy layer.

Using another fabrication approach, Kalathil *et al.* developed a 3D bilayered sponge to address the limitations existing for deep open wounds and chronic conditions like diabetic wounds.[173] The reported system was comprised of a chitosan/GL based hydrogel (CG hydrogel) functionalized with wound-healing peptide (tylotoin)-carrying PLGA nanoparticles (tylotoin-NP) and a top layer based on antibacterial peptide (LLKKK18)-carrying PLLA/chitosan/PHBV nanofibers (LLKKK18-NF) (Fig. 4a). Here, a hydrogel forming solution was dispensed into plastic molds and a preformed electrospun nanofibrous mat was added on the top of the solution. The mold was left undisturbed for crosslinking of the sample at room temperature. A highly porous and elastic structure of this bilayer sponge not only mimicked the ECM but also offered exceptional fluid absorption. It also promoted hemostasis and created an optimal microenvironment for dermal cell survival and migration. It demonstrated notable antibacterial properties while simultaneously facilitating critical wound healing processes such as granulation tissue formation, re-epithelialization, neovascularization, and restoration of skin appendages. The encapsulation efficiency of tylotoin inside PLGA nanoparticles was ≈76.3%. The developed system showed initial burst release of tylotoin followed by sustained release with overall cumulative release of ≈80%. LLKKK18

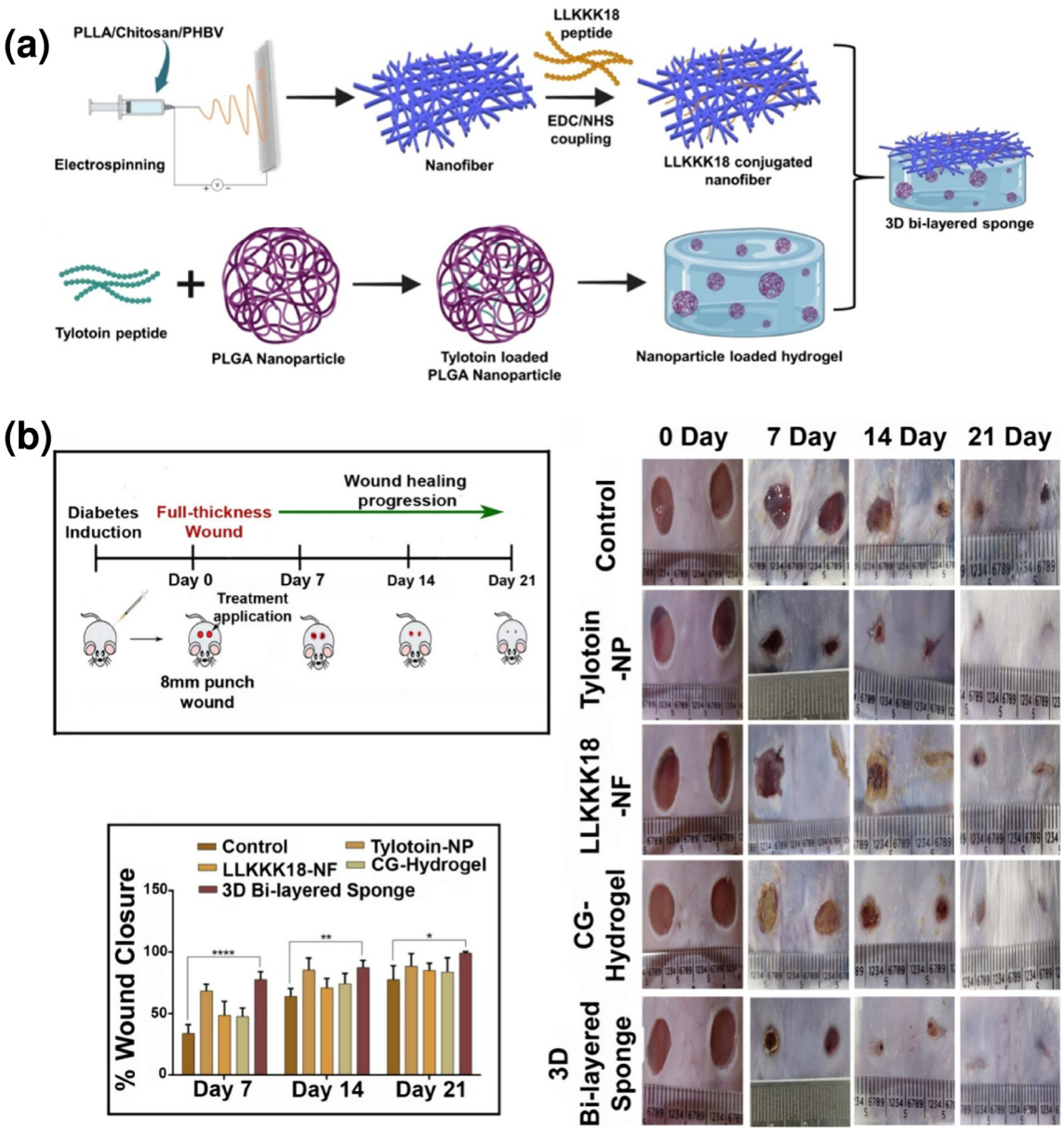

Fig. 4 (a) Fabrication of 3D bilayered sponge by combining antibacterial peptide loaded electrospun nanofibers and the wound tylotoin peptide-entrapped PLGA nanoparticle-loaded hydrogel; (b) wound healing ability of the 3D bilayered sponge dressing in diabetic mice and percentage of wound closure at 7, 14, and 21 days. Results are presented as mean ± SD (n = 5, *P < 0.05). Adapted with permission from[173] Kalathil *et al.* Copyright 2024, American Chemical Society.

release from PLLA/chitosan/PHBV nanofibers was slower and sustained, supporting prolonged antimicrobial activity at the wound site. *In vivo* studies using a diabetic mouse model revealed that the sponge accelerated wound closure, reduced inflammation, and enabled the regeneration of functional skin within three weeks (Fig. 4b). This was marked by mature collagen deposition and reestablishment of skin appendages. It was noted that 3D bilayered sponge demonstrated 87% wound closure in 14 days and complete wound closure by 21 days. The wound closure of the control group in 21 days was 77%, while the wound closure in tylotoin-NP, LLKKK18- NF, and CG-hydrogel was 88%, 85% and 83%, respectively (Fig. 4b).

On the other hand, Chen *et al.* developed a bilayer dressing by casting a Ag/tannic acid-cellulose nanofiber-based hydrogel layer onto vaccarin-loaded polyurethane electrospun nanofibers.[189] The hydrogel layer provided multifunctional properties such as stretchability, antioxidant activity, antifreezing and antidrying resilience, photothermal responsiveness, and antibacterial activity to the dressing. It also demonstrated excellent biocompatibility and controlled drug release behavior. Furthermore, vaccarin release from the nanofibrous layer of the dressing fostered a sustained pro-healing environment over time, while the hydrogel layer acted as a barrier, slowing the rapid release of vaccarin from the nanofibers. Hydrogen bonding and π–π stacking interactions between vaccarin and the hydrogel contributed to the sustained release of vaccarin. Peppas equation was applied to further analyze the release mechanism.

In another approach, Zhang *et al.* fabricated a bilayer wound dressing composed of poly(L-lactate-caprolactone) (PLCL) nanofibers and a keratin hydrogel loaded with a fibroblast growth factor (FGF-2).[174] This dressing was fabricated utilizing a low-pressure filtration-assisted method (Fig. 5a). This approach offered an integrated bilayer structure in which the interface between the hydrogel and electrospun nanofibers was tightly bonded as compared to the simple coating method as observed in SEM images (Fig. 5b). Here, the dermal layer mimicking the keratin hydrogel displayed an exceptional water

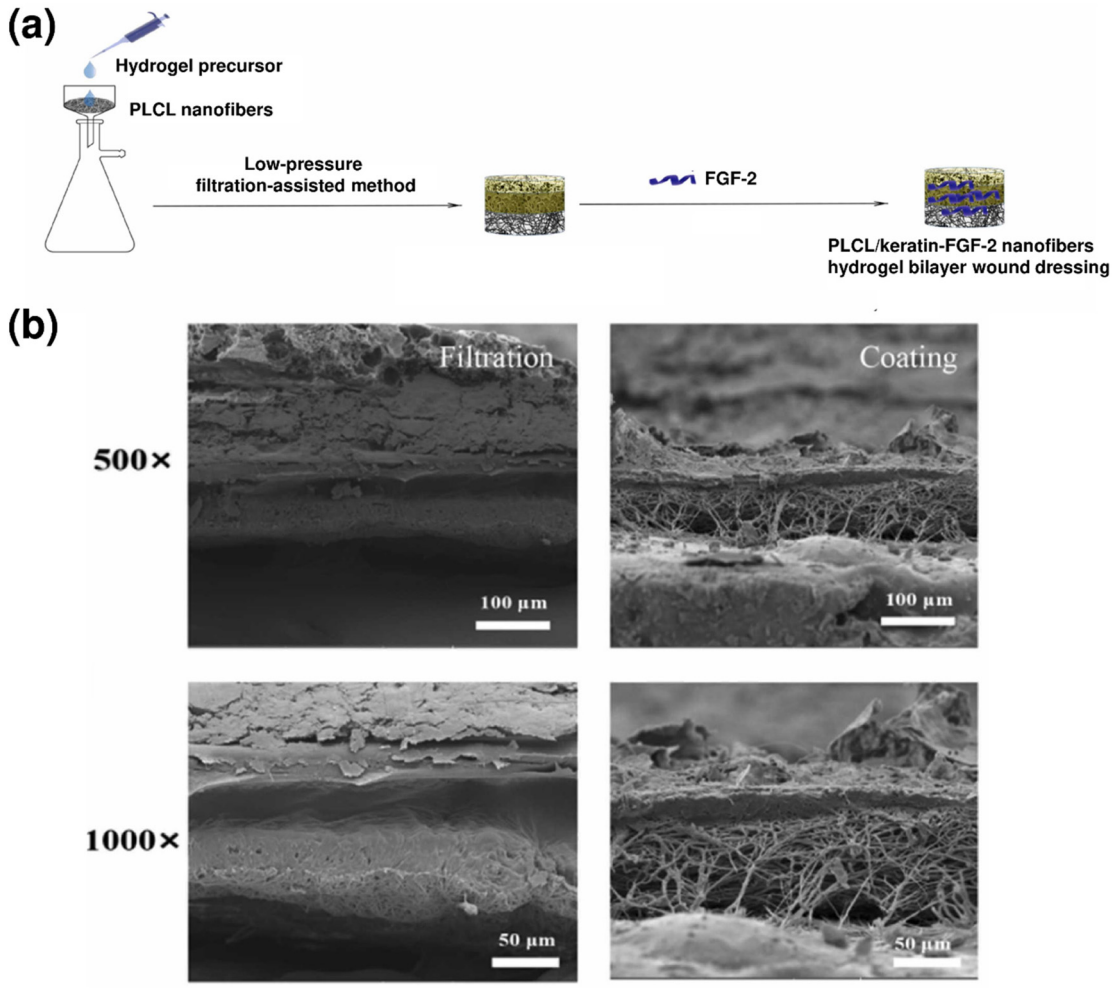

Fig. 5 (a) Schematic representation of the PLCL/keratin-FGF-2 bilayer wound dressing fabricated by using a low-pressure filtration-assisted method; (b) cross-sectional SEM images of the bilayer dressing fabricated by using a low-pressure filtration-assisted method as compared to the coating method at different magnifications. Adapted with permission from[174] Zhang *et al.* Copyright 2022, Elsevier.

absorption capacity of 874% fostering a conducive environment for wound healing. Simultaneously, epidermis layer mimicking PLCL nanofibers exhibited toughness and flexibility which are required for mechanical integrity. *In vivo* studies confirmed its ability to promote re-epithelialization, collagen deposition, regeneration of skin appendages (*e.g.*, hair follicles), angiogenesis, and the recruitment of adipose-derived stem cells (ADSCs). The fabricated bilayer dressing showed a 10.91% loading efficiency of FGF-2, and only 2.37% release of FGF-2 was observed over 120 h. The low loading and release efficiency are limitations of the current design and could be improved through strategies like heparin-mediated FGF-2 loading.

Furthermore, Kolour *et al.* developed a Janus film (Bi-l) composed of electrospun gelatin/PCL nanofibers and a honey/curcumin loaded gelatin-based hydrogel (Fig. 6a).[190] The hydrogel was fabricated using a freeze–thaw method and crosslinked using both physical methods and microbial transglutaminase (Mtg), offering a biocompatible and scalable fabrication process. The fabricated Bi-l showed excellent mechanical properties with a tensile strength of 40 MPa and 70% elongation. Moreover, it also demonstrated a high swelling capacity of 800% and an optimal water vapor transmission rate of 8 g h^{-1} m^{-2}, which are conducive to maintaining a moist wound environment. Drug release studies revealed a sustained release of bioactive agents, with approximately 61% release of curcumin and 66% release of honey over 24 h. *In vitro* studies confirmed the biocompatibility of the materials, with cell viability exceeding 90%. *In vivo* experiments on a rat wound model indicated significantly enhanced wound healing as compared to the control group (NC) and commercial dressings (CS) (Fig. 6b).[190] Furthermore, histological analysis showed excellent re-epithelialization, improved granulation tissue formation, and increased collagen deposition as compared to those of NC and CS (Fig. 6c).[190] Notably, the incorporation of honey and curcumin provided antibacterial, anti-inflammatory, and immune-modulating effects that contributed to the improved healing process.

In another approach, Song *et al.* fabricated a drug-loaded, bilayer wound healing scaffold (PCL-AMX@SG-rhEGF) using a combination of electrospinning and 3D printing techniques (Fig. 7a).[191] The outer layer, composed of PCL nanofibers loaded with amoxicillin (AMX), served as an antibacterial barrier mimicking the epidermis. The inner hydrogel layer (SG) was made from sodium alginate and gelatin incorporated with the recombinant human epidermal growth factor (rhEGF). This inner hydrogel layer was further crosslinked with $CaCl_2$, mimicking the dermis to support tissue regeneration. The scaffold demonstrated favorable mechanical properties, with a tensile modulus of 206.83 ± 32.10 kPa and an elongation at break of 102.09 ± 6.74%. Distinct wettability characteristics were observed, with the outer nanofiber layer being hydrophobic and the inner hydrogel layer being hydrophilic. The fabricated bilayer scaffold showed effective drug release

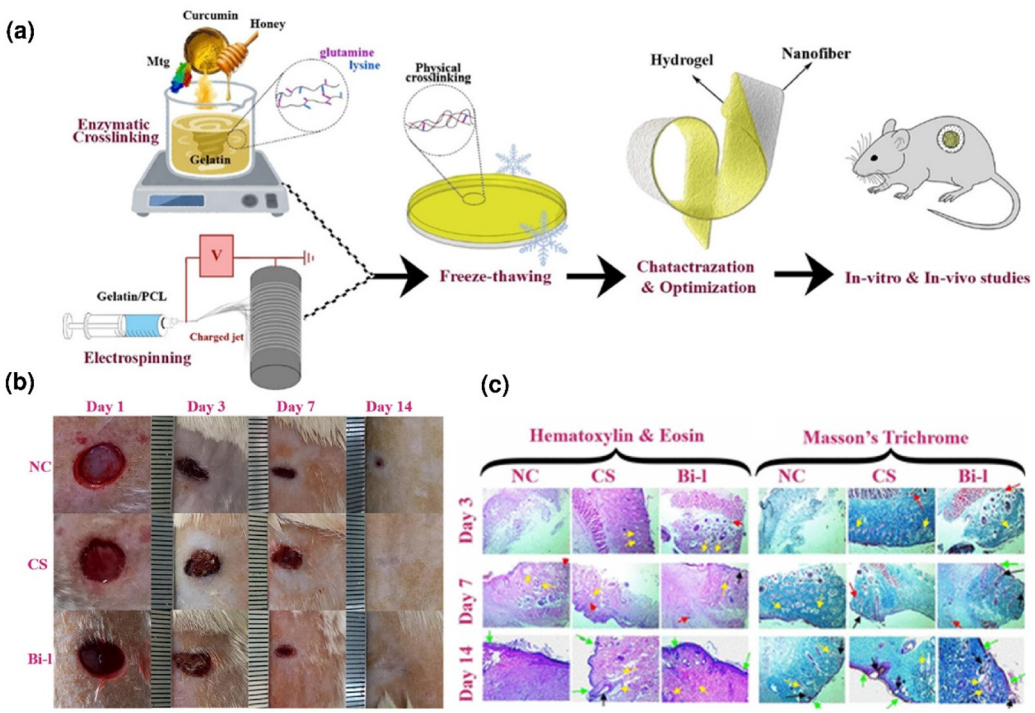

Fig. 6 (a) Fabrication of a Janus film (Bi-l) composed of a physically and enzymatically crosslinked honey/curcumin loaded gelatin hydrogel integrated with electrospun gelatin/PCL nanofibers; (b) evaluation of wound healing in a rat model at 3, 7, and 14 days; and (c) histological analysis of tissue samples at 3, 7, and 14 days. Red, yellow, green, and black arrows represent blood vessels, glands, epidermal layer, and hair follicles, respectively. Adapted with permission from[190] Kolour *et al.* Copyright 2024, American Chemical Society.

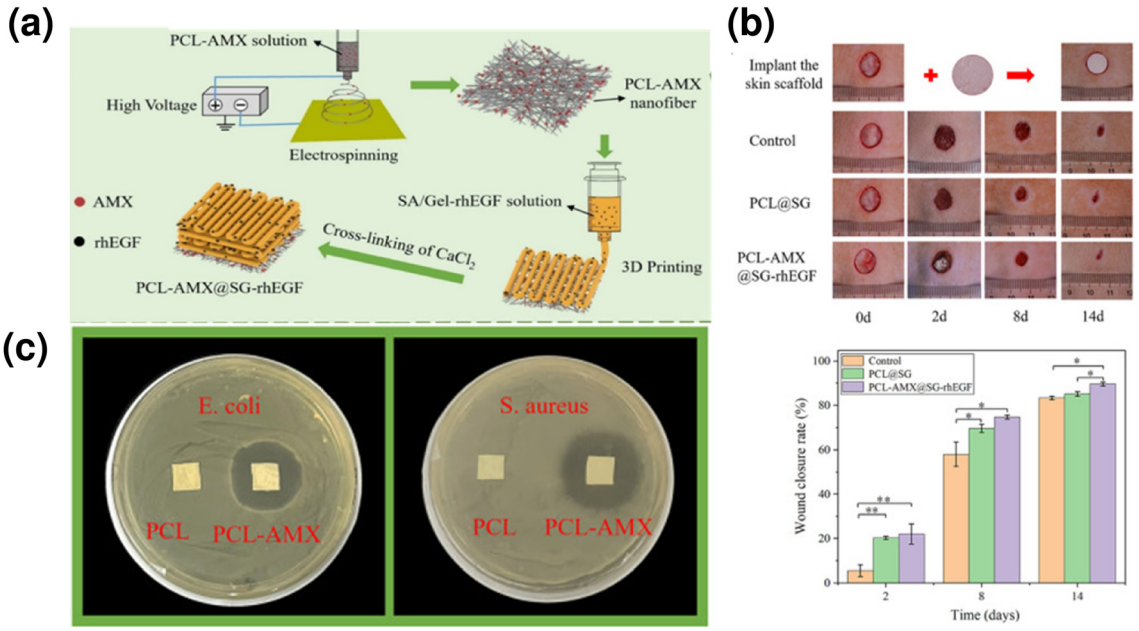

Fig. 7 (a) Fabrication of a bilayer drug-loaded wound healing scaffold (PCL-AMX@SG-rhEGF) using a combination of electrospinning and 3D printing techniques followed by $CaCl_2$ crosslinking; (b) images of wound healing progression in mice treated with the control, PCL@SG, and PCL-AMX@SG-rhEGF scaffolds at 0, 2, 8, and 14 days; and (c) antibacterial activity of PCL and PCL-AMX against *E. coli* and *S. aureus*, showing inhibition zones around PCL-AMX. Adapted with permission from Song *et al.*[191] Copyright 2024, Elsevier.

behavior for both AMX and rhEGF, with an initial burst release in the first 24 h followed by sustained release. AMX was almost completely released within 24 h, and reached a residual concentration of 35.59 ± 1.61 μg mL^{-1} at 240 h. rhEGF followed a similar pattern, with most of the drug released by 72 h and a final concentration of 1048.93 ± 54.10 pg mL^{-1} at 240 h. Moreover, in *in vivo* studies, on day 8, all groups presented outstanding wound healing effects as compared with that on day 2. On day 14, the wound closure rate for the PCL-AMX@SG-rhEGF group reached ≈89%, which was significantly higher as compared to both PCL@SG and control groups (Fig. 7b).[191] Additionally, the antibacterial activity of the PCL-AMX scaffold was evaluated using a zone inhibition method. It showed excellent antibacterial activity against *E. coli* (zone inhibition diameter: 2.85 ± 0.03 mm) and *S. aureus* (zone inhibition diameter: 3.27 ± 0.10 mm) (Fig. 7c).[191]

7. Conclusions and future prospects

Bilayer dressings, combining hydrogel and nanofibrous layers, have emerged as an innovative solution for addressing the challenges associated with the complex wound healing process. These layers produce a synergistic effect collectively, thus improving healing results while diminishing the likelihood of infection and scarring. Here, we have presented a summary of recent advancements in the field of bilayer dressings which includes the integration of bioactive agents (*e.g.*, growth factors, antibacterial agents, natural extracts *etc.*). These additives augment therapeutic potential by promoting angiogenesis, expediting granulation tissue formation, and providing antibacterial features.

Despite the efforts made so far, there are several concerns that need to be tackled for the commercial application of bilayer dressings in the near future. In this direction, optimal mechanical strength and degradation pattern are crucial for wound healing dressings. Although hydrogels possess inherent softness and flexibility, they frequently lack mechanical strength required for their use in high-stress environments. On the other hand, nanofibrous layers may deteriorate at rates that are inconsistent with the healing timeline. Hence, attaining an optimal equilibrium among various physical, chemical, and biological characteristics of both layers is essential for clinical success. Furthermore, in bilayer dressings, the degradation rates of each layer should be strategically tailored to match the wound healing phases and the corresponding therapeutic needs.

A focus should also be placed on stimuli responsive bilayer dressings that can adapt responsively to wound milieu. It allows changes in their structure and physicochemical or mechanical properties in response to external stimuli (*e.g.*, temperature, pH, light *etc.*). It may help in the release of therapeutic agents from the dressing on demand in response to the stimuli. These systems can gain additional advantages through integration with wearable sensors providing unparalleled accuracy in wound management. From a translational standpoint, variability of wound microenvironments (*e.g.*, fluctuating pH, enzyme levels, and moisture) may affect the consistency of the stimuli-responsive behavior and response kinetics may not match the dynamic needs of chronic wounds. Hence, the

stimuli responsive dressings should be designed in such a way that they can adapt to the dynamic wound requirements. Moreover, the biocompatibility of the degradation byproducts of stimuli-responsive systems must be carefully evaluated. Also, large scale production while ensuring cost-effectiveness also presents a considerable challenge. Resolving these issues necessitates collaboration among materials scientists, bioengineers, and clinicians, promoting a multidisciplinary approach to innovation.

Additionally, there exists a significant gap for investigating suitable nanomaterial and natural extract based systems that can enhance the efficacy of bilayer dressings without causing any toxicity. Furthermore, exploring renewable resources for designing bilayer dressings corresponds to sustainable development goals, rendering this a notably appealing area for future investigation.

In conclusion, bilayer dressings that integrate hydrogel and nanofibrous layers have opened a new pathway for efficient wound management. However, this area still requires further innovation and interdisciplinary collaboration to surmount current limitations and make these advanced materials work to their maximum capacity. With further advancement and utilization of emerging technologies, bilayer dressings can facilitate a new era of personalized wound healing therapy.

Author contributions

D. B.: conceptualization and writing – original draft. S. K.: conceptualization and writing – original draft. G. A.: conceptualization, writing – original draft, and writing – review & editing.

Conflicts of interest

There are no conflicts of interest to declare.

Data availability

No primary research results, software or code have been included and no new data were generated or analysed as part of this review.

Acknowledgements

GA is thankful for the financial support from the ANRF Science & Engineering Research Board (SERB-ANRF), India (Grant No. WEA/2023/000001).

References

1 M. Zhang, S. Gong, K. Hakobyan, Z. Gao, Z. Shao, S. Peng, S. Wu, X. Hao, Z. Jiang, E. H. Wong, K. Liang, C. H. Wang, W. Cheng and J. Xu, *Adv. Sci.*, 2024, **11**, 2309006.
2 W. Lopez-Ojeda, A. Pandey, M. Alhajj and A. M. Oakley, Anatomy, skin (integument), in *StatPearls*, StatPearls Publishing, Treasure Island, FL, USA, 2022.
3 M. Li, Y. Liang, J. He, H. Zhang and B. Guo, *Chem. Mater.*, 2020, **32**, 9937–9953.
4 M. Farahani and A. Shafiee, *Adv. Healthcare Mater.*, 2021, **10**, 2100477.
5 R. Laurano, M. Boffito, G. Ciardelli and V. Chiono, *Eng. Regener.*, 2022, **3**, 182–200.
6 X. Zhang, Y. Wang, Z. Gao, X. Mao, J. Cheng, L. Huang and J. Tang, *J. Appl. Polym. Sci.*, 2024, **141**, e54746.
7 G. Ramanathan, L. S. S. Sobhanadhas, G. F. S. Jeyakumar, V. Devi, U. T. Sivagnanam and P. Fardim, *Biomacromolecules*, 2020, **21**, 2512–2524.
8 I. De Luca, P. Pedram, A. Moeini, P. Cerruti, G. Peluso, A. Di Salle and N. Germann, *Appl. Sci.*, 2021, **11**, 1713.
9 Y. Liang, J. He and B. Guo, *ACS Nano*, 2021, **15**, 12687–12722.
10 R. Laurano, M. Boffito, G. Ciardelli and V. Chiono, *Eng. Regener.*, 2022, **3**, 182–200.
11 M. Kharaziha, A. Baidya and N. Annabi, *Adv. Mater.*, 2021, **33**, 2100176.
12 M. G. Nur, M. Rahman, T. M. Dip, M. H. Hossain, N. B. Hossain, S. Baratchi and S. Houshyar, *Wound Repair Regen.*, 2025, **33**, e13233.
13 B. Jia, G. Li, E. Cao, J. Luo, X. Zhao and H. Huang, *Mater. Today Bio*, 2023, **19**, 100582.
14 Y. Xia, S. Yan, H. Wei, H. Zhang, K. Hou, G. Chen, R. Cao and M. Zhu, *ACS Appl. Mater. Interfaces*, 2024, **16**, 34578–34590.
15 G. McKnight, J. Shah and R. Hargest, *Surgery*, 2022, **40**, 8.
16 M. A. Kumar, Physiology of the Skin, in *Techniques in Small Animal Wound Management*, ed. N. J. Buote, John Wiley & Sons, Hoboken, NJ, USA, 2024.
17 O. Jaiyeoba, E. Ogbuju, O. T. Yomi and F. Oladipo, *J. Comput. Theor. Appl.*, 2024, **2**, 22–38.
18 J. A. McGrath and J. Uitto, Structure and Function of the Skin, in *Rook's Textbook of Dermatology*, ed. C. E. M. Griffiths, J. Barker, T. Bleiker, R. Chalmers and D. Creamer, Wiley-Blackwell, Hoboken, NJ, USA, 9th edn, 2023.
19 K. Holte and G. McIntyre, The Skin (Integument): PART I, in *Diseases and Injuries to the Head, Face and Neck: A Guide to Diagnosis and Management*, ed. M. Perry, Springer International Publishing AG, Cham, Switzerland, 2021.
20 B. Li, H. Mei, Z. Zhou, J. Yang, Y. Zhang and F. Qi, *J. Dermatol. Sci. Cosmet. Technol.*, 2024, **1**, 100020.
21 S. Pillai, M. Manco, C. Oresajo and N. Baalbaki, Epidermal Barrier, in *Cosmetic Dermatology: Products and Procedures*, ed. Z. D. Draelos, John Wiley & Sons, Hoboken, NJ, USA, 3rd edn, 2022.
22 S. Benedetti, A. Frosolini, L. Catarzi, A. Marsiglio, P. Gennaro and G. Gabriele, *Healthcare*, 2024, **12**, 501.
23 S. M. Milner, *Eplasty*, 2023, **23**, QA8.
24 O. A. Peña and P. Martin, *Nat. Rev. Mol. Cell Biol.*, 2024, **25**, 599–616.

25 A. Scridon, *Int. J. Mol. Sci.*, 2022, **23**, 12772.
26 M. J. Kuijpers, J. W. Heemskerk and K. Jurk, *Int. J. Mol. Sci.*, 2022, **23**, 5825.
27 A. A. Mamun, C. Shao, P. Geng, S. Wang and J. Xiao, *Front. Immunol.*, 2024, **15**, 1395479.
28 N. N. Mahmoud, K. Hamad, A. Al Shibitini, S. Juma, S. Sharifi, L. Gould and M. Mahmoudi, *ACS Pharmacol. Transl. Sci.*, 2024, **7**, 18–27.
29 A. A. Mamun, C. Shao, P. Geng, S. Wang and J. Xiao, *Front. Immunol.*, 2024, **15**, 1395479.
30 A. A. Mamun, C. Shao, P. Geng, S. Wang and J. Xiao, *Front. Immunol.*, 2024, **15**, 1395479.
31 K. Raziyeva, Y. Kim, Z. Zharkinbekov, K. Kassymbek, S. Jimi and A. Saparov, *Biomolecules*, 2021, **11**, 700.
32 M. Alhajj and A. Goyal, Physiology, Granulation Tissue, in *StatPearls*, StatPearls Publishing, Treasure Island, FL, USA, 2022.
33 M. E. Muse, K. R. Shumway and J. S. Crane, *StatPearls*, StatPearls Publishing, Treasure Island, FL, USA, 2023.
34 P. Viaña-Mendieta, M. L. Sánchez and J. Benavides, *Int. Wound J.*, 2022, **19**, 100–113.
35 A. B. Sousa, A. P. Águas, M. A. Barbosa and J. N. Barbosa, *Regener. Biomater.*, 2022, **9**, rbac065.
36 P. Li, J. Zhang, X. Liu, Z. Xu, X. Zhang, J. Ma, G. Sun and L. Hou, *ACS Appl. Mater. Interfaces*, 2025, **17**, 26156–26177.
37 X. Chen, J. Wang, J. Zhang, H. Lin, M. Tian, M. Li and Y. Tian, *Chem. Eng. J.*, 2024, **486**, 150204.
38 G. I. Taylor, *Proceedings of the Royal Society of London Series A. Mathematical and Physical Sciences*, 1964, **280**, 383–397.
39 L.É Uhljar and R. Ambrus, *Pharmaceutics*, 2023, **15**, 417.
40 D. Ji, Y. Lin, X. Guo, B. Ramasubramanian, R. Wang, N. Radacsi, R. Jose, X. Qin and S. Ramakrishna, *Nat. Rev. Methods Primers*, 2024, **4**, 1.
41 G. R. da Silva, E. Song, K. M. Chen, F. Chen, L. Jiang, H. Kim, N. W. Kang, W. G. Koh and D. Myung, *Int. J. Pharm.*, 2025, **669**, 125009.
42 D. Perumalsami, N. Sabapathi, T. J. Frank, A. Ganesan and J. Rengarajan, *BioNanoScience*, 2024, **15**, 22.
43 S. Goel and Y. Bano, in *Antimicrobial Materials and Coatings*, ed. A. K. Singh, M. Dhayal and C. M. Hussain, Woodhead Publishing, 2025.
44 W. Cao, D. Xia, L. Zhou, Y. Liu, D. Wang, C. Liang and M. Chen, *Mater. Today Phys.*, 2024, **40**, 101316.
45 S. P. Ndlovu, K. S. C. M. Motaung, S. A. Adeyemi, P. Ubanako, L. Ngema, T. Y. Fonkui, D. T. Ndinteh, P. Kumar, Y. E. Choonara and B. A. Aderibigbe, *J. Biomater. Sci., Polym. Ed.*, 2024, **35**, 2380–2401.
46 H. Park, T. V. Patil, S. D. Dutta, J. Lee, K. Ganguly, A. Randhawa, H. Kim and K. T. Lim, *Adv. Healthcare Mater.*, 2024, **13**, 2304114.
47 S. Guo, Y. Ren, R. Chang, Y. He, D. Zhang, F. Guan and M. Yao, *ACS Appl. Mater. Interfaces*, 2022, **14**, 34455–34469.
48 E. Antaby, K. Klinkhammer and L. Sabantina, *Appl. Sci.*, 2021, **11**, 11937.
49 L. V. Hai, L. Zhai, H. C. Kim, P. S. Panicker, D. H. Pham and J. Kim, *Nanomaterials*, 2020, **10**, 1752.
50 R. Lungu, A. Anisiei, I. Rosca, A. I. Sandu, D. Ailincai and L. Marin, *React. Funct. Polym.*, 2021, **167**, 105028.
51 L. Yang, X. Wang, M. Xiong, X. Liu, S. Luo, J. Luo and Y. Wang, *Sci. Rep.*, 2024, **14**, 3942.
52 A. Aldahish, N. Shanmugasundaram, R. Vasudevan, T. Alqahtani, S. Alqahtani, A. M. Asiri, B. Arshad, P. Devanandan, T. Thamaraikani, C. Vellapandian and N. Jayasankar, *Pharmaceuticals*, 2024, **17**, 1305.
53 Y. Wang, L. Chen, D. Y. Ren, Z. X. Feng, L. Y. Zhang, Y. F. Zhong, M. Jin, F. W. Xu, C. Y. Feng, Y. Z. Du and W. Q. Tan, *Mater. Today Bio*, 2022, **15**, 100320.
54 A. Pepe, A. Laezza, F. Armiento and B. Bochicchio, *ChemPlusChem*, 2024, **89**, e202300599.
55 M. H. Psyed, M. M. R. Khan, M. A. K. M. Zahari, M. D. H. Beg and N. Abdullah, *Eur. Polym. J.*, 2023, **197**, 112352.
56 A. Khodabandeh, A. A. Yousefi, S. Jafarzadeh-Holagh and E. Vasheghani-Farahani, *Biomater. Adv.*, 2025, **166**, 214053.
57 T. Saygılı, H. T. Kahraman, G. Aydın, A. Avcı and E. Pehlivan, *Polym. Bull.*, 2024, **81**, 5459–5476.
58 F. Ge, T. Wan, L. Kong, B. Xu, M. Sun, B. Wang, S. Liang, H. Wang and X. Zhao, *Heliyon*, 2024, **10**, e33693.
59 F. Geyik, S. Kaya, D. E. Yılmaz, H. Demirci, İ. Akmayan, T. Özbek and S. Acar, *ACS Omega*, 2024, **9**, 14054–14062.
60 M. Delyanee, A. Solouk, S. Akbari and M. D. Joupari, *Macromol. Biosci.*, 2022, **22**, 2100313.
61 S. Nasser, M. Ibrahim and Y. Atassi, *Mater. Chem. Phys.*, 2021, **267**, 124686.
62 T. Ramamoorthy, A. M. Soloman, D. Annamalai, A. Gopinath, S. Skylab and B. Madhan, *J. Bioact. Compat. Polym.*, 2024, **40**, 31–44.
63 A. Khanbaba, H. Mozaffari, R. Faridi-Majidi and M. A. Derakhshan, *BioNanoScience*, 2024, **15**, 16.
64 C. Li, W. Shang, Y. Huang, J. Ge, J. Ye, X. Qu, Q. Guo, C. Wang, P. Hu and Y. Liu, *Int. J. Biol. Macromol.*, 2025, **285**, 138054.
65 D. Prakashan, A. Singh, A. D. Deshpande, V. Chandra, G. T. Sharma and S. Gandhi, *Int. J. Biol. Macromol.*, 2024, **274**, 133447.
66 C. Cui, S. Sun, X. Li, S. Chen, S. Wu, F. Zhou and J. Ma, *Int. J. Biol. Macromol.*, 2022, **205**, 500–510.
67 L. Zhou, L. Cai, H. Ruan, L. Zhang, J. Wang, H. Jiang, Y. Wu, S. Feng and J. Chen, *Int. J. Biol. Macromol.*, 2021, **183**, 1145–1154.
68 M. A. Derakhshan, N. Nazeri, K. Khoshnevisan, R. Heshmat and K. Omidfar, *J. Diabetes Metab. Disord.*, 2022, **21**, 313–321.
69 Y. Wang, C. Ding, Y. Zhao, J. Zhang, Q. Ding, S. Zhang, N. Wang, J. Yang, S. Xi, T. Zhao, C. Zhao and W. Liu, *Int. J. Biol. Macromol.*, 2023, **252**, 126530.
70 M. Rezaei, M. Nikkhah, S. Mohammadi, S. H. Bahrami and M. Sadeghizadeh, *J. Appl. Polym. Sci.*, 2021, **138**, 50884.

71 B. S. Alotaibi, A. K. Khan, Z. Kharaba, H. Yasin, R. Yasmin, M. Ijaz, M. Khan and G. Murtaza, *ACS Omega*, 2024, **9**, 12825–12834.
72 A. Naeimi, M. Payandeh, A. R. Ghara and F. E. Ghadi, *Carbohydr. Polym.*, 2020, **240**, 116315.
73 M. Abasalta, R. Zibaseresht, M. Y. Zoshk, M. F. Koudehi, M. Irani and Z. Hami, *J. Dispersion Sci. Technol.*, 2023, **44**, 2664–2674.
74 S. Gupta, P. Dutta, V. Acharya, P. Prasad, A. Roy and A. Bit, *J. Bioact. Compat. Polym.*, 2021, **37**, 38–52.
75 C. Wang, Q. Zhang, G. Hou, C. Wang and H. Yan, *Eur. Polym. J.*, 2023, **190**, 112003.
76 A. Asiri, S. Saidin, M. H. Sani and R. H. Al-Ashwal, *Sci. Rep.*, 2021, **11**, 5634.
77 S. Alven, B. Buyana, Z. Feketshane and B. A. Aderibigbe, *Pharmaceutics*, 2021, **13**, 964.
78 A. A. El-Attar, H. B. El-Wakil, A. H. Hassanin, B. A. Bakr, T. M. Almutairi, M. Hagar, B. H. Elwakil and Z. A. Olama, *Membranes*, 2022, **12**, 536.
79 J.-P. Ye, J.-S. Gong, C. Su, Y.-G. Liu, M. Jiang, H. Pan, R.-Y. Li, Y. Geng, Z.-H. Xu and J.-S. Shi, *Colloids Surf., B*, 2020, **194**, 111158.
80 S. Su, T. Bedir, C. Kalkandelen, A. O. Başar, H. T. Şaşmazel, C. B. Ustundag, S. Sengor and O. Gunduz, *Eur. Polym. J.*, 2021, **142**, 110158.
81 B. Singh, J. Kim, N. Shukla, J. Lee, K. Kim and M. H. Park, *ACS Appl. Bio Mater.*, 2023, **6**, 2314–2324.
82 C. Wang, Q. Zhang, G. Hou, C. Wang and H. Yan, *Eur. Polym. J.*, 2023, **190**, 112003.
83 A. Alam, R. Karmakar, A. K. Rengan and M. Khandelwal, *ACS Biomater. Sci. Eng.*, 2023, **9**, 3160–3184.
84 S. Khattak, I. Ullah, M. Sohail, M. U. Akbar, M. A. Rauf, S. Ullah, J. Shen and H. T. Xu, *Aggregate*, 2025, **6**, e688.
85 B. Gautam, M. R. Huang, S. A. Ali, A. L. Yan, H. H. Yu and J. T. Chen, *ACS Appl. Mater. Interfaces*, 2022, **14**, 40322–40330.
86 X. Zhang, R. Lv, L. Chen, R. Sun, Y. Zhang, R. Sheng, T. Du, Y. Li and Y. Qi, *ACS Appl. Mater. Interfaces*, 2022, **14**, 12984–13000.
87 X. Lu, L. Zhou and W. Song, *Polymers*, 2024, **16**, 2596.
88 H. Guo, W. Ran, X. Jin, Y. Huang, F. Long, Y. Xiao, R. Y. Gan, Y. Wu and H. Gao, *Int. J. Biol. Macromol.*, 2024, **278**, 134526.
89 T. Zhao, N. Wang, Y. Wang, J. Yang, Y. Tang, Y. Wang, H. Wei, J. Yang, T. Yu, X. Sun, C. Ding, Q. Li and Y. Yang, *Int. J. Biol. Macromol.*, 2024, **280**, 135724.
90 J. Chen, X. Jia, S. Wang, X. Wang, L. Li, G. Han, Y. Dou and J. Li, *Chem. Eng. J.*, 2024, **497**, 154521.
91 S. Kamalipooya, S. Fahimirad, H. Abtahi, M. Golmohammadi, M. Satari, M. Dadashpour and D. Nasrabadi, *Int. J. Pharm.*, 2024, **653**, 123880.
92 S. Wang, X. Xu, X. Zhu, X. Tan and B. Xie, *ACS Omega*, 2024, **9**, 39472–39483.
93 C. Ding, J. Yang, N. Wang, Q. Ding, S. Sun, Y. Gao, L. Shen, T. Zhao and Y. Wang, *Int. J. Biol. Macromol.*, 2024, **262**, 129937.
94 G. Ajmal, G. V. Bonde, P. Mittal, V. K. Pandey, N. Yadav and B. Mishra, *Mater. Today Commun.*, 2023, **35**, 105633.
95 F. Koohzad and A. Asoodeh, *ACS Appl. Mater. Interfaces*, 2023, **15**, 15172–15184.
96 N. Dehghani, F. Haghiralsadat, F. Yazdian, F. Sadeghian-Nodoushan, N. Ghasemi, F. Mazaheri, M. Pourmadadi and S. M. Naghib, *Int. J. Biol. Macromol.*, 2023, **238**, 124078.
97 G. Pandey, P. Pandey, D. K. Arya, S. Kanaujiya, D. D. Kapoor, R. K. Gupta, S. Ranjan, K. Chidambaram, B. Manickam and P. S. Rajinikanth, *Int. J. Pharm.*, 2023, **638**, 122918.
98 T.-H. Kim, S.-C. Kim, W. S. Park, I.-W. Choi, H.-W. Kim, H. W. Kang, Y.-M. Kim and W.-K. Jung, *Mater. Des.*, 2023, **229**, 111912.
99 Q. Yu, C. Shen, X. Wang, Z. Wang, L. Liu and J. Zhang, *Int. J. Nanomed.*, 2023, **18**, 563–578.
100 C. Liu, Y. Zhu, X. Lun, H. Sheng and A. Yan, *Bioengineered*, 2022, **13**, 4328–4339.
101 T. Liu, Z. Zhang, J. Liu, P. Dong, F. Tian, F. Li and X. Meng, *Int. J. Biol. Macromol.*, 2022, **217**, 998–1011.
102 C. Tan, Z. Yuan, F. Xu and X. Xie, *Cellulose*, 2022, **29**, 3407–3422.
103 H. Motasadizadeh, S. Azizi, A. Shaabani, M. G. Sarvestani, R. Sedghi and R. Dinarvand, *Carbohydr. Polym.*, 2022, **296**, 119956.
104 N. Jirofti, M. Golandi, J. Movaffagh, F. S. Ahmadi and F. Kalalinia, *ACS Biomater. Sci. Eng.*, 2021, **7**, 3886–3897.
105 S. Fahimirad, H. Abtahi, P. Satei, E. Ghaznavi-Rad, M. Moslehi and A. Ganji, *Carbohydr. Polym.*, 2021, **259**, 117640.
106 R. Ramalingam, C. Dhand, V. Mayandi, C. M. Leung, H. Ezhilarasu, S. K. Karuppannan, P. Prasannan, S. T. Ong, N. Sunderasan, I. Kaliappan, M. Kamruddin, V. A. Barathi, N. K. Verma, S. Ramakrishna, R. Lakshminarayanan and K. D. Arunachalam, *ACS Appl. Mater. Interfaces*, 2021, **13**, 24356–24369.
107 M. S. Salami, G. Bahrami, E. Arkan, Z. Izadi, S. Miraghaee and H. Samadian, *BMC Complementary Med. Ther.*, 2021, **21**, 111.
108 S. Hashemikia, F. Farhangpazhouh, M. Parsa, M. Hasan, A. Hassanzadeh and M. Hamidi, *Int. J. Pharm.*, 2021, **597**, 120313.
109 M. Hadizadeh, M. Naeimi, M. Rafienia and A. Karkhaneh, *Mater. Sci. Eng., C*, 2021, **129**, 112362.
110 S. Ahmadi, A. Hivechi, S. H. Bahrami, P. B. Milan and S. S. Ashraf, *Int. J. Biol. Macromol.*, 2021, **173**, 580–590.
111 M. R. El-Aassar, O. M. Ibrahim, M. M. G. Fouda, N. G. El-Beheri and M. M. Agwa, *Carbohydr. Polym.*, 2020, **238**, 116175.
112 H. R. Bakhsheshi-Rad, Z. Hadisi, A. F. Ismail, M. Aziz, M. Akbari, F. Berto and X. B. Chen, *Polym. Test.*, 2020, **82**, 106298.
113 D. Yang, *Chem. Mater.*, 2022, **34**, 1987–1989.
114 Y. Liang, Z. Li, Y. Huang, R. Yu and B. Guo, *ACS Nano*, 2021, **15**, 7078–7093.

115 C. Huang, L. Dong, B. Zhao, Y. Lu, S. Huang, Z. Yuan, G. Luo, Y. Xu and W. Qian, *Clin. Transl. Med.*, 2022, **12**, e1094.
116 C. Xue, X. Xu, L. Zhang, Y. Liu, S. Liu, Z. Liu, M. Wu and Q. Shuai, *Colloids Surf., B*, 2022, **218**, 112738.
117 D. Stan, C. Tanase, M. Avram, R. Apetrei, N.-B. Mincu, A. L. Mateescu and D. Stan, *Exp. Dermatol.*, 2021, **30**, 1218–1232.
118 H. Cao, L. Duan, Y. Zhang, J. Cao and K. Zhang, *Signal Transduction Targeted Ther.*, 2021, **6**, 426.
119 P. Vinchhi, S. U. Rawal and M. M. Patel, in *Drug Delivery Devices and Therapeutic Systems*, ed. E. Chappel, Academic Press, 2021.
120 Z. Ma, A. Nguyen, C. T. C. Chung, D. Mazy, F. Ghezelbash, Z. Yang, Y. Liu, S. Liu, S. Lamer, Z. Gao, F. Obuseh, B. Freedman, M. L. Nault and J. Li, *Adv. Mater. Technol.*, 2024, **9**, 2301594.
121 X. Ma, C. Wang, W. Yuan, X. Xie and Y. Song, *ACS Appl. Polym. Mater.*, 2021, **3**, 6586–6597.
122 J. Chen, J. He, Y. Yang, L. Qiao, J. Hu, J. Zhang and B. Guo, *Acta Biomater.*, 2022, **146**, 119–130.
123 Y. Zhao, D. Wang, T. Qian, J. Zhang, Z. Li, Q. Gong, X. Ren and Y. Zhao, *ACS Nano*, 2023, **17**, 16854–16869.
124 J. Chen, Z. Mu, D. Chen, C. Huang, T. Jin, L. Li, Y. Zeng, Q. Zhou, Y. Zhang, H. Mao, H. Deng, X. Shen, H. Yong and X. Cai, *Chem. Eng. J.*, 2023, **469**, 143985.
125 J. Duarte, F. Mascarenhas-Melo, P. C. Pires, F. Veiga and A. C. Paiva-Santos, *Eur. Polym. J.*, 2024, **211**, 113026.
126 S. Cheng, H. Wang, X. Pan, C. Zhang, K. Zhang, Z. Chen, W. Dong, A. Xie and X. Qi, *ACS Appl. Mater. Interfaces*, 2022, **14**, 11144–11155.
127 Y. Yang, Y. Liang, J. Chen, X. Duan and B. Guo, *Bioact. Mater.*, 2022, **8**, 341–354.
128 H. Cheng, Z. Shi, K. Yue, X. Huang, Y. Xu, C. Gao, Z. Yao, Y. S. Zhang and J. Wang, *Acta Biomater.*, 2021, **124**, 219–232.
129 Z. Xu, G. Liu, J. Huang and J. Wu, *ACS Appl. Mater. Interfaces*, 2022, **14**, 7680–7689.
130 X. Qi, X. Tong, S. You, R. Mao, E. Cai, W. Pan, C. Zhang, R. Hu and J. Shen, *ACS Macro Lett.*, 2022, **11**, 861–867.
131 Y. Wang, K. Liu, W. Wei and H. Dai, *Adv. Funct. Mater.*, 2024, **34**, 2402531.
132 Y. Guo, M. Wang, Q. Liu, G. Liu, S. Wang and J. Li, *Theranostics*, 2023, **13**, 161–196.
133 L. Tan, M. Li, H. Chen, Y. Zhang, Y. Liu, M. Chen, Z. Luo, K. Cai and Y. Hu, *Nano Today*, 2023, **52**, 101962.
134 M. Kamedani, M. Okawa, A. S. Madhavikutty, C.-C. Tsai, A. K. S. Chandel, T. Fujiyabu, N. F. Inagaki and T. Ito, *Biomacromolecules*, 2024, **25**, 1790–1799.
135 A. Zhang, Y. Liu, D. Qin, M. Sun, T. Wang and X. Chen, *Int. J. Biol. Macromol.*, 2020, **164**, 2108–2123.
136 Y. Huang, L. Mu, X. Zhao, Y. Han and B. Guo, *ACS Nano*, 2022, **16**, 13022–13036.
137 J. Cao, P. Wu, Q. Cheng, C. He, Y. Chen and J. Zhou, *ACS Appl. Mater. Interfaces*, 2021, **13**, 24095–24105.
138 J. Thomas, N. Gupta, J. P. Joseph, V. Chopra, A. Pal and D. Ghosh, *ACS Biomater. Sci. Eng.*, 2021, **7**, 5798–5809.
139 D. Nath, J. Ralhan, J. P. Joseph, C. Miglani and A. Pal, *Biomacromolecules*, 2024, **25**, 853–863.
140 J. P. Joseph, N. Gupta, C. Miglani, D. Nath, A. Singh, D. Gupta and A. Pal, *Chem. Mater.*, 2022, **34**, 4364–4374.
141 V. C. Chandran, P. Saha, D. Nath, S. Bera, S. Bhattacharya and A. Pal, *Nanoscale*, 2024, **16**, 13050–13060.
142 C. Lin, Y. Hu, Z. Lin, L. Du, Y. Hu, L. Ouyang, X. Xie, P. Cheng, J. Liao, L. Lu, R. Zeng, P. Xia, Z. Hou, G. Liu and H. Hu, *Bioact. Mater.*, 2025, **43**, 240–254.
143 Y. Liang, M. Li, Y. Yang, L. Qiao, H. Xu and B. Guo, *ACS Nano*, 2022, **16**, 3194–3207.
144 A. Sharma, V. Panwar, B. Mondal, D. Prasher, M. K. Bera, J. Thomas, A. Kumar, N. Kamboj, D. Mandal and D. Ghosh, *Nano Energy*, 2022, **99**, 107419.
145 W. Zhang, L. Liu, H. Cheng, J. Zhu, X. Li, S. Ye and X. Li, *Mater. Adv.*, 2024, **5**, 1364–1394.
146 Y. Liang, J. He and B. Guo, *ACS Nano*, 2021, **15**, 12687–12722.
147 P. Nezhad-Mokhtari, H. Hamishehkar, M. R. Farahpour, A. Mehdipour, R. Rahbarghazi, M. Milani and M. Mehrali, *Chem. Eng. J.*, 2024, **489**, 150992.
148 P. Mahajan, S. Nangare, A. Patil, P. Jain and L. Zawar, *Carbohydr. Polym. Technol. Appl.*, 2024, **7**, 100432.
149 H. Khadim, R. Zeeshan, S. Riaz, S. Tabassum, A. A. Ansari, S. Zulfiqar, M. Yar and A. Asif, *Colloids Surf., A*, 2024, **693**, 134033.
150 E.-R. Kenawy, M. A. El-Meligy, Z. S. Ghaly, M. E. Kenawy and E. A. Kamoun, *J. Polym. Environ.*, 2024, **32**, 2140–2157.
151 S. A. Sideek, H. B. El-Nassan, A. R. Fares, N. A. Elkasabgy and A. N. ElMeshad, *Pharmaceutics*, 2024, **16**, 90.
152 Y. Han, Z. Yin, Y. Wang, Y. Jiang, J. Chen, Z. Miao, F. He, R. Cheng, L. Tan and K. Li, *Biomacromolecules*, 2024, **25**, 2587–2596.
153 J. Li, Y. Li, C. Guo and X. Wu, *Chem. Eng. J.*, 2024, **481**, 148458.
154 G. P. Rajalekshmy, R. M. Ramesan, C. S. Geetha, K. V. Pratheesh, S. J. Shenoy and T. V. Anilkumar, *ACS Biomater. Sci. Eng.*, 2024, **10**, 2552–2566.
155 R. Abdel-Gawad, R. Osman, G. A. S. Awad and N. Mortada, *Carbohydr. Polym.*, 2024, **324**, 121526.
156 V. Singh, D. K. Tripathi, V. K. Sharma, D. Srivastava, U. Kumar, K. M. Poluri, B. N. Singh, D. Kumar and V. Kumar R, *J. Mol. Struct.*, 2023, **1286**, 135548.
157 Q. Li, S. Zhang, R. Du, Y. Yang, Y. Liu, Z. Wan and X. Yang, *ACS Appl. Mater. Interfaces*, 2023, **15**, 17562–17576.
158 N. Rashid, S. H. Khalid, I. U. Khan, Z. Chauhdary, H. Mahmood, A. Saleem, M. Umair and S. Asghar, *ACS Omega*, 2023, **8**, 7575–7586.
159 W. Tan, T. Long, Y. Wan, B. Li, Z. Xu, L. Zhao, C. Mu, L. Ge and D. Li, *Carbohydr. Polym.*, 2023, **312**, 120824.
160 Y. He, K. Liu, S. Guo, R. Chang, C. Zhang, F. Guan and M. Yao, *Acta Biomater.*, 2023, **155**, 199–217.

161 N. Raina, S. Haque, H. S. Tuli, A. Jain, P. Slama and M. Gupta, *ACS Omega*, 2023, **8**, 34995–35011.
162 M. Dong, Y. Mao, Z. Zhao, J. Zhang, L. Zhu, L. Chen and L. Cao, *Int. Wound J.*, 2022, **19**, 679–691.
163 Y. Tian, P. Guan, C. Wen, M. Lu, T. Li, L. Fan, Q. Yang, Y. Guan, X. Kang, Y. Jiang, C. Ning, R. Fu, G. Tan and L. Zhou, *ACS Appl. Mater. Interfaces*, 2022, **14**, 54488–54499.
164 Y. Wang, L. Chen, D.-Y. Ren, Z.-X. Feng, L.-Y. Zhang, Y.-F. Zhong, M.-Y. Jin, F.-W. Xu, C.-Y. Feng, Y.-Z. Du and W.-Q. Tan, *Mater. Today Bio*, 2022, **15**, 100320.
165 M. Li, Y. Liang, Y. Liang, G. Pan and B. Guo, *Chem. Eng. J.*, 2022, **427**, 132039.
166 R. Gharibi, A. Shaker, A. Rezapour-Lactoee and S. Agarwal, *ACS Biomater. Sci. Eng.*, 2021, **7**, 3633–3647.
167 M.-P. Tian, A.-D. Zhang, Y.-X. Yao, X.-G. Chen and Y. Liu, *Carbohydr. Polym.*, 2021, **261**, 117878.
168 F. R. Diniz, R. C. A. P. Maia, L. R. M. de Andrade, L. N. Andrade, M. V. Chaud, C. F. da Silva, C. B. Corrêa, R. L. C. de Albuquerque Junior, L. Pereira da Costa, S. R. Shin, S. Hassan, E. Sanchez-Lopez, E. B. Souto and P. Severino, *Nanomaterials*, 2020, **10**, 390.
169 G. Singh, A. Nayal, S. Malhotra and V. Koul, *Carbohydr. Polym.*, 2020, **247**, 116757.
170 L. Yang, Z. Han, C. Chen, Z. Li, S. Yu, Y. Qu and R. Zeng, *Mater. Sci. Eng., C*, 2020, **117**, 111265.
171 S. E. Maloney, K. V. McGrath, M. J. R. Ahonen, D. S. Soliman, E. S. Feura, H. R. Hall, S. M. Wallet, R. Maile and M. H. Schoenfisch, *Biomacromolecules*, 2021, **22**, 867–879.
172 X. Han, L. Wang, Y. Shang, X. Liu, I.-K. Kang, J. Shen and J. Yuan, *J. Mater. Chem. B*, 2023, **11**, 1008–1019.
173 N. C. Kalathil, M. R. Shah, V. C. Lailakumari, P. Prabhakaran, H. Kumarapilla and G. S. V. Kumar, *ACS Appl. Bio Mater.*, 2024, **7**, 6492–6505.
174 M. Zhang, S. Xu, C. Du, R. Wang, C. Han, Y. Che, W. Feng, C. Wang, S. Gao and W. Zhao, *Colloids Surf., B*, 2023, **222**, 113119.
175 Y. Wu, M. Li, R. He, L. Xiao, S. Liu, K. Chen, H. Qiang, K. Ji, L. Li, Y. Yin, X. Yuan, M. Li, J. Gao and Y. Li, *Chem. Eng. J.*, 2024, **485**, 149545.
176 Y. Chen, R. Li, B. Li, K. Li and Y. Hao, *Int. J. Biol. Macromol.*, 2024, **261**, 129751.
177 Z. Li, X. Xing, C. Zhao, Q. Wu, J. Liu, X. Qiu and L. Wang, *Carbohydr. Polym.*, 2024, **333**, 121991.
178 C. Gao, L. Zhang, J. Wang, M. Jin, Q. Tang, Z. Chen, Y. Cheng, R. Yang and G. Zhao, *J. Mater. Chem. B*, 2021, **9**, 3106–3130.
179 L. Wu, Y. Wang, X. Zhao, T. Zhao, J. Li, Y. Kuang, Y. He, S. Yang, Z. Gu and H. Mao, *J. Nanobiotechnol.*, 2025, **23**, 448.
180 Y. Wang, Y. Xu, W. Zhai, Z. Zhang, Y. Liu, S. Cheng and H. Zhang, *Nat. Commun.*, 2022, **13**, 5056.
181 X. Liu, L. Gao, S. Fu, W. Zhao, F. Wang, J. Gao, C. Li, H. Wu and L. Wang, *Mater. Des.*, 2023, **227**, 111706.
182 X. Wang, P. Xue, S. Ma, Y. Gong and X. Xu, *ACS Appl. Mater. Interfaces*, 2023, **15**, 49689–49700.
183 H. Zhong, Z. Zhang, M. Wang, Y. Fang, K. Liu, J. Yin, J. Wu and J. Du, *Biomater. Sci.*, 2025, **13**, 697–710.
184 M. Shahriari-Khalaji, M. Sattar, R. Cao and M. Zhu, *Bioact. Mater.*, 2023, **29**, 177–195.
185 M. Alizadeh, S. Salehi, M. Tavakoli, M. Mirhaj, J. Varshosaz, N. Kazemi, S. Salehi, M. Mehrjoo and S. A. M. Abadi, *Int. J. Biol. Macromol.*, 2023, **233**, 123491.
186 M. Mirhaj, M. Tavakoli, J. Varshosaz, S. Labbaf, S. Salehi, A. Talebi, N. Kazemi, V. Haghighi and M. Alizadeh, *Carbohydr. Polym.*, 2022, **292**, 119648.
187 R. Khan, M. U. A. Khan, G. M. Stojanović, A. Javed, S. Haider and S. I. A. Razak, *ACS Omega*, 2024, **9**, 6527–6536.
188 M. Tavakoli, M. Mirhaj, J. Varshosaz, M. H. Al-Musawi, Y. Q. Almajidi, A. M. D. Pajooh, M. Shahriari-Khalaji, F. Sharifianjazi, M. Alizadeh, S. Labbaf, K. E. Shahrebabaki, P. M. Nasab, M. Firuzeh and S. N. Esfahani, *ACS Appl. Mater. Interfaces*, 2023, **15**, 55276–55286.
189 Y. Chen, Y. Zhang, A. Mensaha, D. Li, Q. Wang and Q. Wei, *Carbohydr. Polym.*, 2021, **255**, 117508.
190 A. K. Kolour, S. Ghoraishizadeh, M. S. Zaman, A. Alemzade, M. Banavand, J. Esmaeili and M. Shahrousvand, *ACS Appl. Bio Mater.*, 2024, **7**, 8642–8655.
191 Y. Song, Q. Hu, S. Liu, Y. Wang, H. Zhang, J. Chen and G. Yao, *Int. J. Biol. Macromol.*, 2024, **275**, 129705.

